was related to both the size of the HbV and the increasing composite viscosity of the plasma suspension consisting in original hamster blood plasma, Dx70 molecules, and HbV, and which resulted in a shift of oxygen delivery in favor of the collateralized, ischemic and hypoxic flap tissue.

Additional studies will be necessary to outline the influence of both HbV concentration and viscosity of the solutions, and the long-term benefit of the observed improvement in oxygenation would yet have to be confirmed by evaluating the functionality and survival of the jeopardized tissue. Moreover, our data may not be extrapolated to ischemic conditions in other, vital organs, such as the myocardium or cerebral tissue, in which the oxygen demand is substantially higher than in the present flap tissue.

In summary, we conclude that up to a 50% blood exchange, normovolemic hemodilution with HbV-Dx70 solutions led to a dose- and oxygen affinity-dependent improvement of oxygenation in the ischemic, hypoxic flap tissue, which was not related to the oxygen-carrying capacity of the circulating blood. Thus our study strongly emphasizes the potential function of HbVs as a therapeutic that may be used to improve the delivery of oxygen to ischemic and hypoxic tissues, which exceeds its role as a simple RBC substitute.

DISCLOSURES

This research was supported by Swiss National Foundation for Scientific Research Grants 32-054092.98 (to D. Erni) and 32-050771.97 (to M. Leunig), by the Department of Clinical Research, University of Berne, Switzerland, and by Health Sciences Research, Research on Advanced Medical Technology, Artificial Blood Project, Grant 12090101 from the Ministry of Health, Labour and Welfare, Japan.

REFERENCES

1. **Chang TM.** Oxygen carriers. *Curr Opin Investig Drugs* 3: 1187–1190, 2002.
2. **Chowdary RP, Berkower AS, Moss ML, and Hugo NE.** Fluorocarbon enhancement of skin flap survival in rats. *Plast Reconstr Surg* 79: 98–101, 1987.
3. **Cole DJ, Drummond JC, Patel PM, Nary JC, and Applegate RL 2nd.** Effect of oncotic pressure of diaspirin cross-linked hemoglobin (DCLHb) on brain injury after temporary focal cerebral ischemia in rats. *Anesth Analg* 83: 342–347, 1996.
4. **Erni D, Sakai H, Banic A, Tschopp HM, and Intaglietta M.** Quantitative assessment of microhemodynamics in ischemic skin flap tissue by intravital microscopy. *Ann Plast Surg* 43: 405–415, 1999.
5. **Erni D, Sakai H, Tsai AG, Banic A, Sigurdsson GH, and Intaglietta M.** Haemodynamics and oxygen tension in the microcirculation of ischaemic skin flaps after neural blockade and haemodilution. *Br J Plast Surg* 52: 565–572, 1999.
6. **Erni D, Wettstein R, Schramm S, Contaldo C, Sakai H, Takeoka S, Tsuchida E, Leunig M, and Banic A.** Normovolemic hemodilution with Hb vesicle solution attenuates hypoxia in ischemic hamster flap tissue. *Am J Physiol Heart Circ Physiol* 284: H1702–H1709, 2003.
7. **Falthfull NS, Fennema M, and Erdmann W.** Protection against myocardial ischaemia by prior haemodilution with fluorocarbon emulsions. *Br J Anaesth* 60: 773–778, 1988.
8. **Intaglietta M.** Microcirculatory basis for the design of artificial blood. *Microcirculation* 6: 247–258, 1999.
9. **Intaglietta M and Tompkins WR.** Microvascular measurements by video image shearing and splitting. *Microvasc Res* 5: 309–312, 1973.
10. **Jahr JS, Nesargi SB, Lewis K, and Johnson C.** Blood substitutes and oxygen therapeutics: an overview and current status. *Am J Ther* 9: 437–443, 2002.
11. **Kavdia M, Pittman RN, and Popel AS.** Theoretical analysis of effects of blood substitute affinity and cooperativity on organ oxygen transport. *J Appl Physiol* 93: 2122–2188, 2002.
12. **Kerger H, Saltzman DJ, Menger MD, Messmer K, and Intaglietta M.** Systemic and subcutaneous microvascular P_{O_2} dissociation during 4-h hemorrhagic shock in conscious hamsters. *Am J Physiol Heart Circ Physiol* 270: H827–H836, 1996.
13. **Leunig M, Demhartner TJ, Sckell A, Fraitzl CR, Gries N, Schenk RK, and Ganz R.** Quantitative assessment of angiogenesis and osteogenesis after transplantation of bone: comparison of isograft and allograft bone in mice. *Acta Orthop Scand* 70: 374–380, 1999.
14. **McCarthy MR, Vandegriff KD, and Winslow RM.** The role of facilitated diffusion in oxygen transport by cell-free hemoglobins: implications for the design of hemoglobin-based oxygen carriers. *Biophys Chem* 92: 103–117, 2001.
15. **Mirhashemi S, Ertefai S, Messmer K, and Intaglietta M.** Model analysis of the enhancement of tissue oxygenation by hemodilution due to increased microvascular flow velocity. *Microvasc Res* 34: 290–301, 1987.
16. **Nishide H, Chen XS, and Tsuchida E.** Facilitated oxygen transport with modified and encapsulated hemoglobins across non-flowing solution membrane. *Artif Cells Blood Substit Immobil Biotechnol* 25: 335–346, 1997.
17. **Page TC, Light WR, McKay CB, and Hellums JD.** Oxygen transport by erythrocyte/hemoglobin solution mixtures in an in vitro capillary as a model of hemoglobin-based oxygen carrier performance. *Microvasc Res* 55: 54–64, 1998.
18. **Powanda DD and Chang TM.** Cross-linked polyhemoglobin-superoxide dismutase-catalase supplies oxygen without causing blood-brain barrier disruption or brain edema in a rat model of transient global brain ischemia-reperfusion. *Artif Cells Blood Substit Immobil Biotechnol* 30: 23–37, 2002.
19. **Premaratne S, Harada RN, Chun P, Suehiro A, and McNamara JJ.** Effect of perfluorocarbon exchange transfusion on reducing myocardial infarct size in a primate model of ischemia-reperfusion injury: a prospective, randomized study. *Surgery* 117: 670–676, 1995.
20. **Sakai H, Hara H, Yuasa M, Tsai AG, Takeoka S, Tsuchida E, and Intaglietta M.** Molecular dimensions of Hb-based O_2 carriers determine constriction of resistance arteries and hypertension. *Am J Physiol Heart Circ Physiol* 279: H908–H915, 2000.
21. **Sakai H, Suzuki Y, Kinoshita M, Takeoka S, Maeda N, and Tsuchida E.** Oxygen release from Hb-vesicles: comparison with red blood cells and acellular Hb solution using an artificial oxygen permeable narrow tube with 28 μm inner diameter (Abstract). *Artif Blood* 11: 113, 2003.
22. **Sakai H, Takeoka S, Park SI, Kose T, Hamada K, Izumi Y, Yoshizu A, Nishide H, Kobayashi K, and Tsuchida E.** Surface modification of hemoglobin vesicles with poly(ethyleneglycol) and effects on aggregation, viscosity, and blood flow during 90% exchange transfusion in anesthetized rats. *Bioconjug Chem* 8: 15–22, 1997.
23. **Sakai H, Takeoka S, Wettstein R, Tsai AG, Intaglietta M, and Tsuchida E.** Systemic and microvascular responses to hemorrhagic shock and resuscitation with Hb vesicles. *Am J Physiol Heart Circ Physiol* 283: H1191–H1199, 2002.
24. **Sakai H, Tsai AG, Rohlfs RJ, Hara H, Takeoka S, Tsuchida E, and Intaglietta M.** Microvascular response to hemodilution with Hb vesicles as red blood cell substitutes: influence of O_2 affinity. *Am J Physiol Heart Circ Physiol* 276: H552–H562, 1999.
25. **Schramm S, Wettstein R, Wessendorf R, Jakob SM, Banic A, and Erni D.** Acute normovolemic hemodilution improves oxygenation in ischemic flap tissue. *Anesthesiology* 96: 1478–1484, 2002.

26. **Schumacker PT, Suggett AJ, Wagner PD, and West JB.** Role of hemoglobin P_{50} in O_2 transport during normoxic and hypoxic exercise in the dog. *J Appl Physiol* 59: 749–757, 1985.
27. **Stein CJ and Ellsworth ML.** Capillary oxygen transport during severe hypoxia: role of hemoglobin oxygen affinity. *J Appl Physiol* 75: 1601–1607, 1993.
28. **Sunder-Plassmann L, Klövekorn WP, Holper K, Hase U, and Messmer K.** The physiological significance of acutely induced hemodilution. In: *Proc 6th Eur Conf Microcirculation*, edited by Ditzel J and Lewis DH. Basel, Switzerland: Karger, 1971, p. 23–28.
29. **Sutherland GR, Farrar JK, and Peerless SJ.** The effect of Fluosol on oxygen availability in focal cerebral ischemia. *Stroke* 15: 829–835, 1984.
30. **Tsai AG, Friesenecker B, McCarthy M, Sakai H, and Intaglietta M.** Plasma viscosity regulates capillary perfusion during extreme hemodilution in hamster skinfold model. *Am J Physiol Heart Circ Physiol* 275: H2170–H2180, 1998.
31. **Vadapalli A, Goldman D, and Popel AS.** Calculations of oxygen transport by red blood cells and hemoglobin solutions in capillaries. *Artif Cells Blood Substit Immobil Biotechnol* 30: 157–188, 2002.

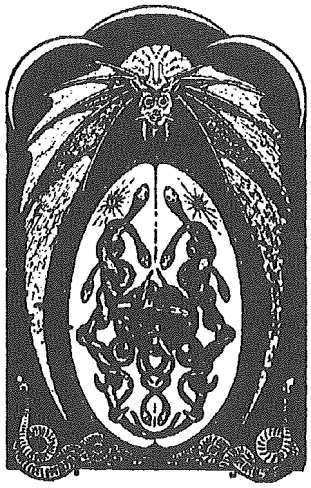

Am J Physiol Heart Circ Physiol 285: H2543–H2551, 2003.
First published July 24, 2003; 10.1152/ajpheart.00537.2003.

O_2 release from Hb vesicles evaluated using an artificial, narrow O_2-permeable tube: comparison with RBCs and acellular Hbs

Hiromi Sakai,[1] Yoji Suzuki,[2] Megumi Kinoshita,[2] Shinji Takeoka,[1] Nobuji Maeda,[2] and Eishun Tsuchida[1]

[1]*Advanced Research Institute for Science and Engineering, Waseda University, Tokyo 169-8555; and*
[2]*Department of Physiology, School of Medicine, Ehime University, Shigenobu, Ehime 791-0295, Japan*

Submitted 11 June 2003; accepted in final form 21 July 2003

Sakai, Hiromi, Yoji Suzuki, Megumi Kinoshita, Shinji Takeoka, Nobuji Maeda, and Eishun Tsuchida. O_2 release from Hb vesicles evaluated using an artificial, narrow O_2-permeable tube: comparison with RBCs and acellular Hbs. *Am J Physiol Heart Circ Physiol* 285: H2543–H2551, 2003. First published July 24, 2003; 10.1152/ajpheart.00537.2003.—A phospholipid vesicle that encapsulates a concentrated hemoglobin (Hb) solution and pyridoxal 5′-phosphate as an allosteric effector [Hb vesicle (HbV) diameter, 250 nm] has been developed to provide an O_2 carrying ability to plasma expanders. The O_2 release from flowing HbVs was examined using an O_2-permeable, fluorinated ethylenepropylene copolymer tube (inner diameter, 28 μm) exposed to a deoxygenated environment. Measurement of O_2 release was performed using an apparatus that consisted of an inverted microscope and a scanning-grating spectrophotometer with a photon-count detector, and the rate of O_2 release was determined based on the visible absorption spectrum in the Q band of Hb. HbVs and fresh human red blood cells (RBCs) were mixed in various volume ratios at a Hb concentration of 10 g/dl in isotonic saline that contained 5 g/dl albumin, and the suspension was perfused at the centerline flow velocity of 1 mm/s through the narrow tube. The mixtures of acellular Hb solution and RBCs were also tested. Because HbVs were homogeneously dispersed in the albumin solution, increasing the volume of the HbV suspension resulted in a thicker marginal RBC-free layer. Irrespective of the mixing ratio, the rate of O_2 release from the HbV/RBC mixtures was similar to that of RBCs alone. On the other hand, the addition of 50 vol% of acellular Hb solution to RBCs significantly enhanced the rate of deoxygenation. This outstanding difference in the rate of O_2 release between the HbV suspension and the acellular Hb solution should mainly be due to the difference in the particle size (250 vs. 7 nm) that affects their diffusion for the facilitated O_2 transport.

blood substitutes; red blood cells; hemoglobin; microcirculation; oxygenation; liposome

VARIOUS KINDS OF HEMOGLOBIN (Hb)-based O_2 carriers (HBOCs) have been developed for the substitution of the function of red blood cells (RBCs) including intramolecularly cross-linked, polymerized, polymer-conjugated, and liposome-encapsulated Hbs (LEHs; Refs. 6, 42). Historically, it has been regarded that the O_2 affinity (expressed as P_{50}; the O_2 tension at which Hb is half-saturated with O_2) should be regulated similar to that of RBCs, namely, ~25–30 Torr, using an allosteric effector or by a direct chemical modification of the Hb molecules. Theoretically, this allows sufficient O_2 unloading during blood microcirculation as can be evaluated by the arteriovenous difference in O_2 saturation (So_2) in accordance with an O_2 equilibrium curve. It has been expected that decreasing O_2 affinity (increasing P_{50}) results in an increase in O_2 unloading. This is supported by the result in a mouse model (31) that RBCs with a high P_{50} value show enhanced O_2 release for improved exercise capacity.

The size of HBOCs is much smaller than that of RBCs. Thus even if the O_2 affinity of both O_2 carriers is similar in the equilibrated condition, the O_2 releasing and binding rates should be different depending on the flow conditions of the carriers and the diffusion of O_2. In a stopped-flow analyses, significantly faster O_2 release rates for an unmodified Hb solution or LEHs rather than RBCs were confirmed (e.g., O_2 dissociation rate constant, 84 s^{-1} for unmodified Hb solution vs. 4.4 s^{-1} for RBCs; Refs. 8, 30, 45). However, these observations were performed under homogeneous conditions and at dilute (<10 μM) Hb concentrations ([Hb]), and it was not clear whether this significant difference would actually be observed in the in vivo condition and how the microcirculation would respond to the difference.

O_2 transfer from blood to tissues in the microcirculatory network is the result of a complex process whereby a substantial fraction of O_2 is exchanged in the arterioles and venules (10, 11, 14) where RBCs are not homogeneously distributed. RBCs tend to move to the centerline in laminar flow, and there is a plasma layer in the marginal zone as is clearly demonstrated in microvessels (17). For this reason, studies of O_2 release in microvessels as well as in capillaries are physiologically important (14, 34, 38, 39, 43). Therefore, the O_2 release rates under more physiological conditions, at a higher [Hb], and in flow conditions in

Address for reprint requests and other correspondence: E. Tsuchida, Advanced Research Institute for Science and Engineering, Waseda Univ., Tokyo 169-8555, Japan (E-mail: eishun@waseda.jp).

The costs of publication of this article were defrayed in part by the payment of page charges. The article must therefore be hereby marked "*advertisement*" in accordance with 18 U.S.C. Section 1734 solely to indicate this fact.

microvessels have been required for discussion of the dynamics of the O_2 releasing that couples with tissue oxygenation. The measurement can be performed using an artificial, narrow, O_2-permeable tube (35). In the case of blood, a cell-free plasma layer between a RBC-flow column and a vessel wall and a highly viscous Hb solution inside RBCs could be barriers to the O_2 diffusion. On the other hand, HBOCs are so small that they are homogeneously dispersed in the plasma phase. Page et al. (20) demonstrated using an artificial flow channel excavated in an O_2-permeable silicone rubber film that a polymerized bovine Hb showed facilitated O_2 release when the Hb was mixed with RBCs.

Phospholipid vesicles that encapsulate concentrated Hb have been developed [Hb vesicles (HbVs) or LEHs; diameter, 250 nm] as another type of HBOC that possesses a cell structure similar to RBCs (21, 24–30, 42). Both RBCs and HbVs have a lipid-bilayer membrane that prevents direct contact of Hb with blood components and endothelial lining. Furthermore, Hb encapsulation in the vesicle suppresses hypertension induced by vasoconstriction; this mechanism is presumably due to the effects of free Hb, which scavenges the endogenous vasorelaxation factors, nitric oxide, and carbon monoxide (13, 24) due to their high affinity with Hb. In this report, we evaluate for the fist time (based on microscopic observations) the O_2 unloading profile of our HbVs compared with RBCs and an acellular unmodified Hb solution using an artificial, narrow, O_2-permeable tube with a 28-μm inner diameter. This methodology has been well established by Tateishi et al. (35, 36).

MATERIALS AND METHODS

Preparation of HbVs, Hb solutions, and an RBC suspension. The HbVs were prepared under sterile conditions as previously reported (24, 27, 32, 33). Hb was purified from outdated donated blood obtained from the Hokkaido Red Cross Blood Center (Sapporo, Japan) and the Japanese Red Cross Society (Tokyo). The encapsulated purified Hb (38 g/dl) contained 17.6 mM of pyridoxal 5′-phosphate (PLP; Sigma; St. Louis, MO) as an allosteric effector at a molar PLP/Hb ratio of 2.5. The lipid bilayer was composed of a mixture of 1,2-dipalmitoyl-*sn*-glycero-3-phosphatidylcholine, cholesterol, and 1,5-*O*-dihexadecyl-*N*-succinyl-L-glutamate in a 5:5:1 molar ratio (Nippon Fine Chemical; Osaka, Japan). The surface of the HbVs was modified with polyethylene glycol (PEG; 5,000 mol wt) using 1,2-distearoyl-*sn*-glycero-3-phosphatidylethanolamine-*N*-polyethylene glycol (NOF; Tokyo; 0.3 mol% of total lipids). HbV diameter was 252 ± 53 nm (determined by the light-scattering method). The P_{50} value was 28 Torr at 37°C, which was measured with a Hemox analyzer (TCS Medical Products; Huntingdon Valley, PA). HbVs were resuspended in either 5 g/dl recombinant human serum albumin (HSA; 69,000 mol wt; Nipro; Osaka; HbV_{HSA}) or in 6 g/dl hydroxylethyl starch (HES; 70,000 mol wt; Kyorin Chemistry Lab; Tokyo; HbV_{HES}), and the final [Hb] was adjusted to 10 g/dl.

The purified Hb solution (38 g/dl) was diluted with a phosphate-buffered saline to 10 g/dl, and PLP was added at a molar Hb/PLP ratio of 1:3 or 1:1. Under these conditions, the P_{50} values were 29 and 15 Torr, respectively, and these Hb solutions were termed Hb29 and Hb15, respectively. Fresh human RBCs were obtained from a healthy donor (Y. Suzuki). RBCs were washed twice with isotonic saline and suspended in the saline that contained 5 g/dl HSA, and the [Hb] was adjusted to 10 g/dl. The RBC suspension was used within a day of the blood collection. The physicochemical properties of all O_2 carriers are summarized in Table 1. The viscosities of the suspensions were measured with either a capillary rheometer (oscillatory capillary rheometer OCR-D; Anton Paar; Graz, Austria) or a cone-plate viscometer (model E; Tokyo Keiki; Tokyo) at 37°C and at the shear rates of 300 and 71 s^{-1}. The latter shear rate is approximately identical to the wall shear rate of the narrow tube (inner diameter, 28 μm) as performed in the present study when the centerline velocity is 1 mm/s. The HbV or Hb solutions were mixed with the RBC suspension at volume ratios of 0:100, 10:90, 50:50, 90:10, and 100:0. For example, the mixture of 10 vol% HbV_{HSA}s and 90 vol% RBCs is abbreviated as $10HbV_{HSA}$/90RBC for convenience.

Perfusion of HbV/RBC or Hb/RBC mixtures through narrow tubes. Narrow, O_2-permeable tubes (inner diameter, 28.1 or 28.6 μm; wall thickness, 37.5 μm; length, 150 mm) were produced from a fluorinated ethylenepropylene copolymer at Hirakawa Hewtech (Ibaraki, Japan) as described by Kubota et al. (16). One end of the narrow tube was connected to a reservoir of the HbV/RBC or Hb/RBC suspension. The narrow tube was placed horizontally between two wide acrylic plates with a short gap (~2 mm) on the stage of an inverted microscope (IMT-2; Olympus Optics; Tokyo). The suspension in the reservoir was gently and continuously mixed with a magnetic stirrer. The gap between the two acrylic plates was filled with nitrogen-bubbled saline that contained 10 mM sodium hydrosulfite ($Na_2S_2O_4$; Wako Pure and Fine Chemical; Tokyo). The narrow tube was not permeable to sodium hydrosulfite. The HbVs distributed homogeneously in the narrow tube so that it was difficult to determine the marginal HbV-free layer. Therefore, the thickness of the marginal RBC-free layer, the distance between the tube inner wall and a nearest RBC, was measured at 50 points using an image-processing technique (35), and the values were averaged. The perfusion pressure was monitored with a sensor (P-231D; Nihon Kohden; Tokyo) equipped with an amplifier (AP-601G; Nihon Kohden). The entire perfusion experiment was performed at 25°C.

Table 1. *Physicochemical properties of Hb solutions and HbV and RBC suspensions*

	Hb15	Hb29	HbV_{HSA}	HbV_{HES}	RBC
[Hb], g/dl	10	10	10	10	10
Hb/PLP	1:1	1:3	1:2.5	1:2.5	
P_{50}, Torr	15	29	28	28	28
Diameter, nm	7	7	252 ± 53	252 ± 53	~8,000
Suspending medium	Saline	Saline	5 g/dl HSA	6 g/dl HES	5 g/dl HSA
Viscosity					
cP at 300 s^{-1}	1	1	3.5	5.1	3.0
cP at 71 s^{-1}	1	1	3.9	5.7	3.9

Values are means ± SD for diameter measurements of hemoglobin (Hb) vesicles (HbV). Hb and HbV viscosity was measured with a capillary viscometer; red blood cell (RBC) viscosity was measured with a cone-plate viscometer. Hb15 and Hb29, purified Hb with P_{50} values of 15 and 29 Torr, respectively; HbV_{HSA} and HbV_{HES}, HbVs suspended with human serum albumin (HSA) or hydroxylethyl starch (HES), respectively; [Hb], Hb concentration; PLP, pyridoxal 5′-phosphate.

Measurement of So_2 in narrow tubes. The apparatus (35) consisted of an inverted microscope with an objective lens of ×40 magnification (ULWD CDPlan 40PL; Olympus Optics), a scanning-grating spectrophotometer with a sensitive photon-counting detector that counted 1×10^3 to 3×10^6 photons/s (USP-410; Unisoku; Osaka), and a computer (PC-386V; Epson; Tokyo). The light intensity of a halogen lamp in the microscope was controlled by a current stabilizer (NLO 18-10; Takasago; Tokyo). The spectrophotometer was connected to the microscope eyepiece through a thin light guide (diameter, 0.4 mm) made of quartz and was operated by the computer. The grating was scanned in 508 steps over the wavelength range of 499.2–600.8 nm with a gate time of 20 ms/step for photon counting; data were obtained every 0.2 nm. One visible spectrum from a 5-μm-diameter spot over the centerline of the narrow tube was recorded within 20 s. A measuring spot on the narrow tube within the visual field of the microscope was fixed on a monitor (PVM-1371; Sony; Tokyo) through a video camera attached to the vertical eyepiece (DXC-930; Sony) by sliding the stage of the microscope and/or by rotating the cylindrical mirror. The centerline flow velocity was determined using the cross-correlation technique (2, 15), and the velocity was adjusted to 1.0 mm/s by changing the pressure applied to the reservoir of HbV/RBC or Hb/RBC mixtures. Under these conditions, the Reynolds number was 0.025 and the laminar flow was theoretically established.

The spectroscopic measurements were performed at traveling distances of 15, 30, 50, 80, and 100 mm. After a steady flow of RBCs and a steady oxygenation state of the flowing RBCs and HbVs (or Hbs) were attained a few minutes later, 10 scans were accumulated. Numerical filtering was then applied with a moving average of 5 successive values (e.g., absorbances at 499.6, 499.8, 500.0, 500.2, and 500.4 nm) in the scanning step to obtain a smoothed absorption spectrum (used to improve the signal-to-noise ratio). One scan of RBCs flowing in the narrow tube showed a remarkable deviation in absorbance values (Fig. 1*A*). On the other hand, HbVs showed less deviation due to the homogeneous dispersion of the vesicles. The accumulation of 10 scans followed by the moving averaging of 5 successive values in the scanning step of every 0.2 nm provided a smooth spectrum even for the RBC suspension (Fig. 1*B*). However, owing to the light scatter by fine particles, the absorbance of the HbVs at a shorter wavelength was slightly higher than that at a longer wavelength (29).

In the spectra of the 100%-deoxygenated and 100%-oxygenated HbVs, two isosbestic points (522 and 586 nm; Ref. 44) in the Q band of Hb were connected by a straight line as the baseline (Fig. 1*C*). The absorbances at 555 nm (ΔA_{555}, λ_{max} of deoxyHb) and 576 nm (ΔA_{576}, λ_{max} of oxyHb) from the baseline were obtained to make a calibration line that shows the relationship between the So_2 (in %) and the ratio of the two absorbances ($R = \Delta A_{555}/\Delta A_{576}$) as $So_2 = (35 - 15R)/(0.25R + 0.21)$. The So_2 values of each sample were plotted versus the traveling distance.

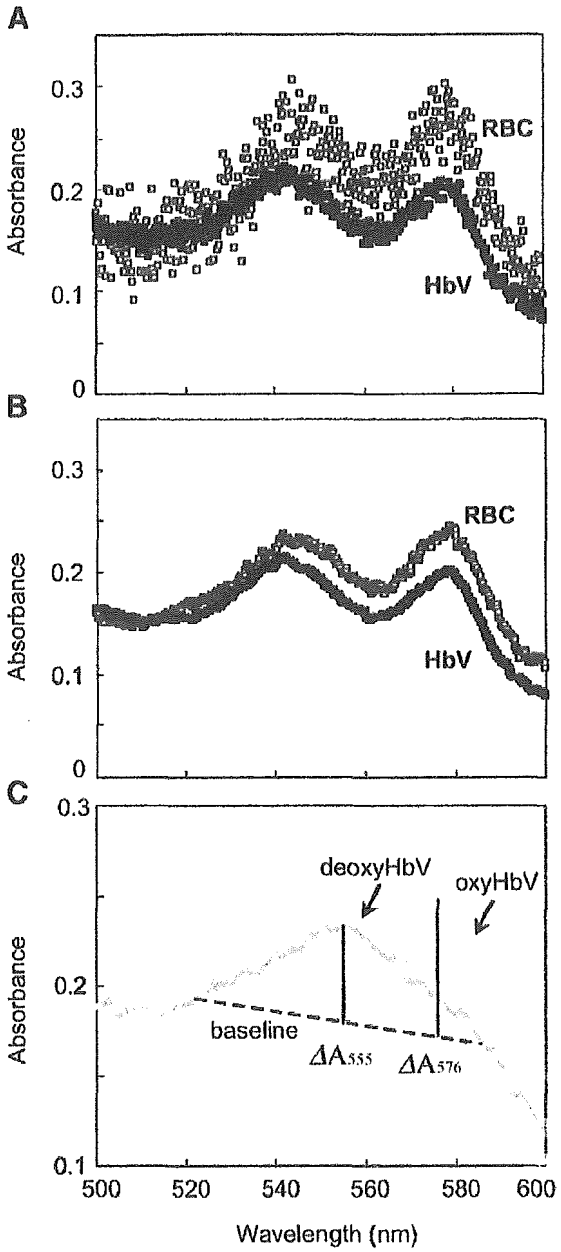

Fig. 1. *A*: one scan of the red blood cell (RBC) suspension showed a significantly scattered spectrum, whereas hemoglobin (Hb) vesicles (HbVs) showed a smooth spectrum. *B*: accumulation of 10 scans followed by the moving average of 5 successive values (using a 0.2-nm scanning step) provided enough resolution to calculate the O_2 saturation (So_2). *C*: for So_2 determination, two isobestic points of the spectra of deoxygenated (deoxy-) and oxygenated (oxy)HbVs (at 522 and 586 nm) were connected by a straight line (baseline). On the basis of the absorbances at 555 (ΔA_{555}, λ_{max} of deoxyHb) and 576 (ΔA_{576}, λ_{max} of oxyHb) nm from the baseline, a relationship between So_2 and the ratio of the two absorbances ($R = \Delta A_{555}/\Delta A_{576}$) was expressed as So_2 (in %) = $(35 - 15R)/(0.25R + 0.21)$.

RESULTS

Flow patterns of HbV/RBC mixtures in narrow tube. Figure 2 shows a microscopic view of the mixtures of RBCs and HbV_{HSA}s flowing in the narrow tubes. The thickness of the RBC-free marginal layer increased with increasing mixing ratio of HbV_{HSA}, and the layer seemed to be slightly turbid and dark colored due to the presence of HbV particles with a 250-nm diameter (29). The thickness of the RBC-free layer was 2.7 ± 1.7 μm for RBCs alone (100RBC), 3.5 ± 1.8 μm for $10HbV_{HSA}$/90RBC, 4.8 ± 2.2 μm for $50HbV_{HSA}$/50RBC, and 7.0 ± 1.6 μm for $90HbV_{HSA}$/10RBC. On the other hand, the mixture of RBCs and the Hb solution produced a transparent layer, but the distribution of RBCs was not

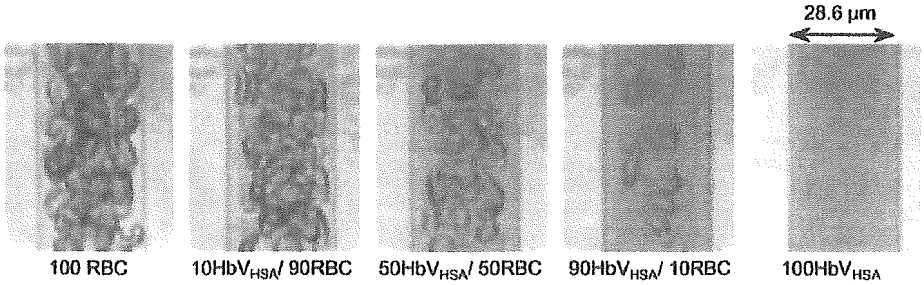

Fig. 2. Flow patterns of RBCs mixed with HbVs suspended in recombinant human serum albumin (HbV_{HSA}/RBC) in a narrow tube. HbV particles were homogeneously dispersed in a suspension medium. They tended to distribute in the marginal zone of the flow. Thickness of the RBC-free layer increased with increasing amount of HbV_{HSA}. RBC-free phase became darker and more semitransparent, which indicates the presence of HbVs. Tube diameter, 28 μm; Hb concentration ([Hb]), 10 g/dl; centerline flow velocity, 1 mm/s.

changed significantly compared with the HbV/RBC mixtures (data not shown).

Perfusion pressure of narrow tube. The perfusion pressure of the RBC suspension mixed with HbV_{HSA}, HbV_{HES}, or Hb29 in various ratios was examined at the constant centerline flow velocity of 1 mm/s (Fig. 3). The addition of the Hb29 solution to the RBC suspension in HSA (3.9 cP; Table 1) decreased the perfusion pressure from 10 kPa (100RBC) to 6 kPa (90Hb29/10RBC) due to the lower viscosity of the Hb solution (1.3 cP at 71 s^{-1}). On the other hand, the addition of HbVs increased the perfusion pressure in proportion to the HbV/RBC mixing ratio. Especially, the perfusion pressure (41 kPa) of the mixture of 90% HbV_{HES}s (5.7 cP; Table 1) and 10% RBC (3.9 cP) was more than four times higher than that of RBCs alone (10 kPa).

Spectroscopic changes of HbV/RBC and Hb/RBC mixtures. Figure 4 shows the representative spectroscopic changes of the mixtures of RBCs with HbVs or Hbs at various traveling distances in the narrow tubes. The most significant change was observed for the mixture of 90 vol% Hb29 solution and 10 vol% RBCs (90Hb29/10RBC). Two characteristic peaks of oxyhemoglobin in the Q band significantly decreased with traveling distance, and at 100 mm, the two peaks were flattened. On the other hand, the 90HbV$_{HSA}$/10RBC mixture showed slight changes, but the changes were almost identical to those observed for the 100RBC suspension. The addition of 10 vol% Hb29s to 90 vol% RBCs (to make 10Hb29/90RBC) did not seem to significantly change the spectrum.

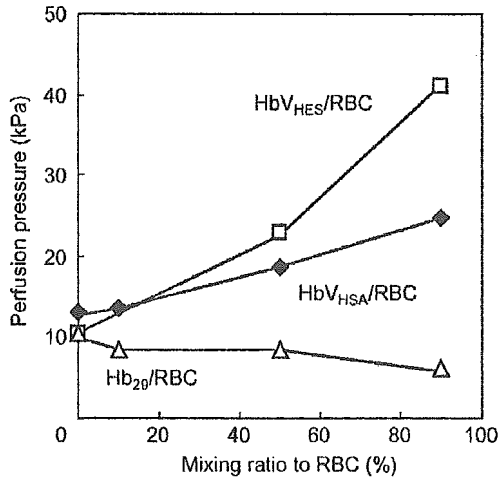

Fig. 3. Perfusion pressure measurements of RBCs mixed with HbV_{HSA} (HbV_{HSA}/RBC), hydroxylethyl starch (HbV_{HES}/RBC), or purified Hb and added pyridoxal 5′-phosphate (PLP), which has a P_{50} value of 29 Torr (Hb29/RBC). [Hb] flowing in the narrow tube, 10 g/dl; centerline flow velocity, 1 mm/s.

O_2 release from HbV/RBC mixtures. According to the calibration line for the So_2, the So_2 values (in %) were plotted vs. the traveling distances. Figure 5 summarizes the O_2 release from the HbV/RBC mixtures in various mixing ratios. The rates of O_2 release from all the mixtures were similar to that of 100RBC, and ~40% of the O_2 was released at the traveling distance of 100 mm.

The influence of the suspending medium of HbV on O_2 release was compared using HbV_{HSA} and HbV_{HES} in the mixture of 90 vol% HbVs and 10 vol% RBCs (Fig. 6). Irrespective of the suspending medium (HSA and HES), the rates of O_2 release were almost identical for the two mixtures.

O_2 release from Hb/RBC mixtures. Contrary to the results with the HbV/RBC mixtures, the Hb/RBC mixtures showed faster O_2 release rates than RBCs alone at the mixing ratio of 50 vol% for Hb29 and 90 vol% for both Hb29 and Hb15 (Fig. 7). The Hb29 (P_{50} = 29 Torr) possessed a similar P_{50} value as HbV (P_{50} = 30 Torr; Table 1). The 10Hb29/90RBC mixture did not show any apparent change in the O_2 release compared with RBCs alone. However, the addition of 50Hb29/50RBC clearly showed a faster O_2 release. The 90Hb29/10RBC mixture showed a much faster release rate, and 55% of the O_2 was released at the 100-mm traveling distance. Addition of Hb15, which has a higher O_2 affinity (P_{50} = 15 Torr), also enhanced the O_2 release, but the enhancement was less than that of Hb29 as evaluated for the 50Hb15/50RBC mixture. However, at the mixing ratios of 10 and 90 vol%, there were no apparent differences in enhancement of O_2 unloading between Hb15 and Hb29.

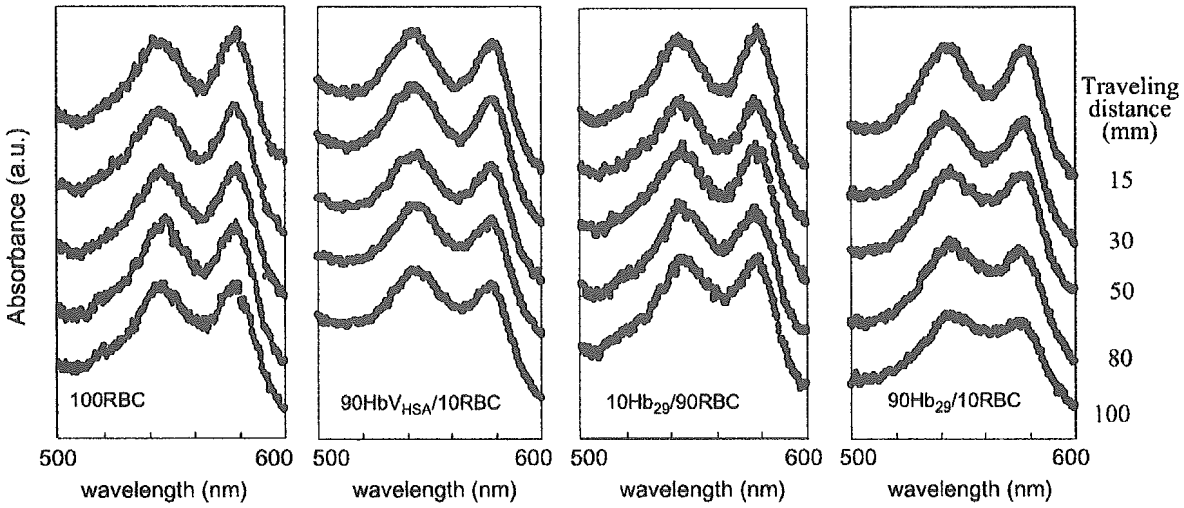

Fig. 4. Representative spectroscopic changes in Q bands of 100% RBCs and various HbV$_{HSA}$/RBC and Hb29/RBC mixtures compared with traveling distance in the narrow tube. Mixture of 90% Hb29 with 10% RBCs (90Hb29/10RBC) showed significant reduction in the two characteristic peaks attributed to oxyHb. Mixtures shown: 90HbV$_{HSA}$/10RBC, 90% HbV$_{HSA}$ mixed with 10% RBCs; 10Hb29/90RBC, 10% Hb29 mixed with 90% RBCs.

DISCUSSION

The principal finding of this study using the narrow O_2-permeable tube is that the rate of O_2 release from HbVs is similar to that from RBCs at a constant [Hb] of 10 g/dl. On the other hand, acellular, unmodified Hb showed faster O_2 release rates. This property of HbVs is outstanding compared with previous findings for O_2 release rates measured by the stopped-flow method. The stopped-flow analysis confirmed that HbVs released O_2 significantly faster than RBCs and slower than acellular, unmodified Hbs (30). Vandegriff and Olson (45) also examined the O_2 release of RBCs of different sizes (diameter, 4.32–50 μm) from various species and of LEHs (diameter, 200 nm, which is similar in size to HbVs). They clarified that the O_2 release rate depended primarily on the cell surface area-to-volume ratio and the intracellular [Hb] and that LEHs had the fastest release rate. These discrepancies of the results between the perfusion study using the O_2-permeable tube and the stopped-flow methods should be mainly due to the differences in the experimental conditions. The stopped-flow studies were performed with homogeneous solutions at the low [Hb] of 10 μM (0.065 g/dl) in a mixing cuvette in which the dissociated O_2 immediately diminished with sodium hydrosulfite and the O_2 gradient between intra- and extracellular compartments was extremely high. In the present study using the O_2-permeable tube, the [Hb] was as high as 1.6 mM (10 g/dl) with a high viscosity, and a certain kind of O_2 gradient between the center of the tube and the tube wall would be formed. Therefore, the present experimental conditions were much closer to the in vivo physiological conditions, although the wall of the narrow tube was unavoidably thick.

We confirmed under our experimental conditions that acellular, unmodified Hb shows a much faster O_2 unloading rate than RBCs as reported by other researchers (18, 20). The differences in the rates between

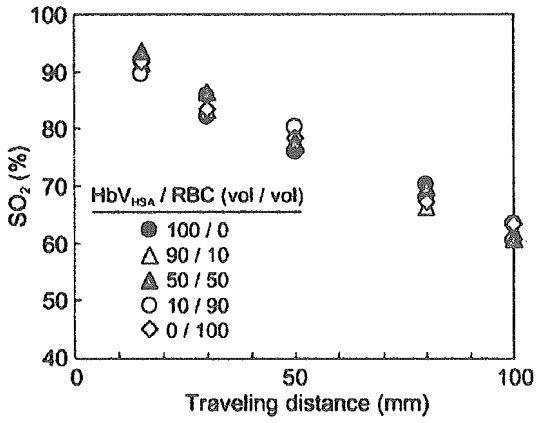

Fig. 5. O_2 release from the HbV$_{HSA}$/RBC mixture for different mixing ratios determined at various traveling distances.

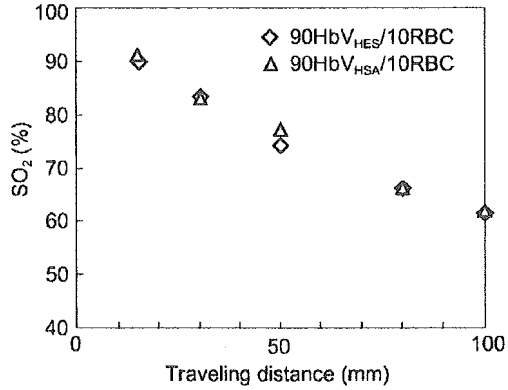

Fig. 6. Effects of suspending media on O_2 release from HbV/RBC mixture: comparison of 90HbV$_{HSA}$/10RBC and 90% HbV$_{HES}$ with 10% RBCs (90HbV$_{HES}$/10RBC) determined at various traveling distances.

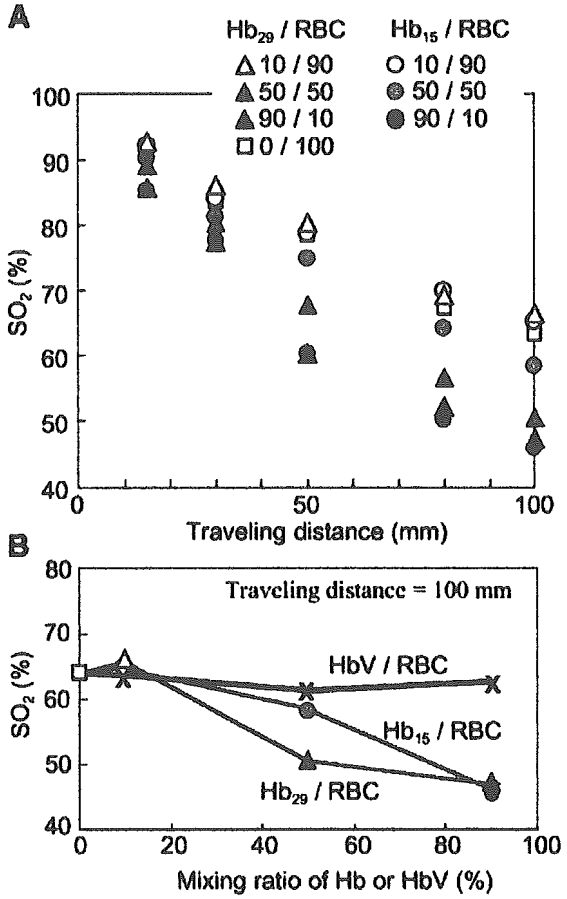

Fig. 7. *A*: effects of O_2 affinity on O_2 release from Hb/RBC mixtures at various traveling distances: comparison of Hb29/RBC and Hb15/RBC mixtures of various ratios. *B*: effects of Hb/RBC or HbV/RBC mixing ratios on S_{O_2}: data from *A* for Hb/RBC and from Fig. 5 for HbV/RBC at the traveling distance of 100 mm. Hb15, purified Hb with pyridoxal 5′-phosphate (PLP) added, which has a P_{50} value of 15 Torr.

the acellular Hb and HbVs could be explained by the theory of facilitated O_2 transport by the diffusion of O_2-bound Hb molecules (1, 5, 7). The total O_2 flux is the sum of the fluxes of free O_2 molecules and O_2 bound as HbO_2. The diffusion of HbO_2 contributes to the facilitated O_2 transport. According to the Stokes-Einstein equation, the diffusion constant (D_{HbO_2}) is defined as

$$D_{HbO_2} = \frac{k \cdot T}{6 \cdot \pi \cdot \eta \cdot r} \quad (1)$$

where k is the Boltzman constant and T is absolute temperature. This equation demonstrates that the diffusion of a macromolecule, i.e., the contribution of facilitated O_2 diffusion, is inversely proportional to the viscosity of the solution (η) and the radius of the macromolecule (r); therefore, the contribution of facilitated O_2 diffusion is inversely proportional to the size of the carriers and the viscosity (18).

Nishide et al. (19) studied O_2 diffusion across a nonflowing solution membrane, and they found that the presence of Hb molecules in a solution (<30 g/dl) significantly facilitated O_2 transport. When comparing HbVs, unmodified human Hb (HbAo), and polymerized Hbs, the "apparent" D_{HbO_2} values are in the following order: HbAo (9×10^{-7} cm^2/s) > polyHbs (2×10^{-7} cm^2/s) > HbVs (3.5×10^{-8} cm^2/s) at [Hb] = 10 g/dl, with solution viscosity values ($1.0 < 1.8 < 3.2$ cP, respectively) and molecular sizes ($7 < \sim 15 < 200$ nm, respectively) that are in inverse order in accordance with *Eq. 1*. As a result, facilitated O_2 transport is significantly reduced for the suspension of HbVs.

According to the study of McCarthy et al. (18), a PEG-conjugated Hb (PEG-Hb) shows a similar O_2 release rate with RBCs in an artificial microflow channel, whereas the acellular cross-linked Hbs and HbAo show faster rates. The PEG chains should not be a barrier layer to the O_2 release. The main difference in the O_2 release between PEG-Hb and other acellular Hbs should be due to the diffusion of Hb and the viscosity: PEG-Hb has a larger molecular size (28 vs. 7 nm) and a higher viscosity (3.2 vs. 0.9 cP) than the Hb molecule. These properties of PEG-Hb may reduce the O_2 unloading, because the diffusion constant of PEG-Hb should be lower than that of an unmodified Hb. The higher O_2 affinity of PEG/Hb (P_{50} = 10 Torr) should also contribute to the slower O_2 unloading, because we confirmed that the Hb15/RBC mixture showed a slower O_2 unloading than did the Hb29/RBC mixture at a 50:50 mixing ratio. Attention should be paid to the theory that facilitated O_2 transport ([O_2] facilitated) decreases with increasing P_{50} according to (1, 19)

$$[O_2] \text{ facilitated} \propto \frac{[Hb]_0 \cdot D_{Hb}}{1/K + Po_2} \quad (2)$$

where $[Hb]_0$ is the total [Hb], Po_2 is the O_2 partial pressure, D_{Hb} is the diffusion coefficient of Hb, and K is the equilibrium constant of the O_2 binding reaction (its reciprocal is proportional to the P_{50} value). Accordingly, the faster O_2 release rate for Hb29 than for Hb15 is not due to the higher level of facilitated O_2 transport but is simply a result of the lower O_2 affinity.

When a large amount of HbV is exchange transfused, the addition of a plasma expander is required, because the oncotic pressure of the HbV suspension is close to zero (26). HbV_{HES} shows a higher viscosity (5.7 cP at 71 s^{-1}) compared with HbV_{HSA} (3.9 cP), because the interaction of HbV particles with extended HES chains is possibly stronger than that with globular HSA molecules. Using the optical microscope, however, we could not observe the HbV aggregates in the suspension; this was possibly due to the low molecular weight of HES (70,000). The marginal RBC-free layer formed by axial accumulation of RBCs is important for the maintenance of blood flow as a lubricating layer (3). The addition of HbV_{HSA} to RBCs increased the thickness of the RBC-free layer from 2.7 ± 1.7 (100RBC) to 7.0 ± 1.6 μm (90HbV_{HSA}/10RBC). This increase was due to preferential flow of smaller particles, HbVs, near the peripheral region of the flow channel (4) and reduction of RBCs (i.e., reduction of hematocrit) (31). Furthermore, the perfusion pressure was increased at a con-

stant flow rate, because the addition of the viscous HbV_{HES} and HbV_{HSA} suspensions increased the viscosity of the RBC-free lubricating layer. The increase in the perfusion pressure was more evident for the more viscous HbV_{HES} than for HbV_{HSA} possibly owing to the differences in the molecular conformations of HES and HSA; also, differences in their concentrations also partly contributed to the perfusion pressure values (37). Despite the viscosity difference between the two suspensions, O_2 release rates from the RBC mixtures were not significantly altered in the present experimental conditions. It has been confirmed (35) that the diffusion constant of the O_2 molecule is not significantly influenced by medium viscosity. The medium viscosity may influence the flow behavior of HbVs in a narrow tube. However, a homogeneous distribution of HbV_{HES} and HbV_{HSA} in the narrow tube was observed by cross-sectional scanning of the narrow tube during flow, and the vesicle-free layer was hardly observed in the marginal region. Therefore, homogeneous distribution of HbVs in the narrow tube and the identical O_2 affinity of the vesicles provided identical O_2 release rates from HbV_{HES} and HbV_{HSA} under a constant flow velocity. This phenomenon also supports the fact that the contribution of HbVs to facilitated O_2 transport by diffusion of HbVs is significantly lower than acellular Hbs; thus viscosity does not influence O_2 unloading. We conclude that under the present experimental conditions, differences in medium viscosity affect the perfusion pressure but not the O_2 release from HbVs and/or RBCs.

The low contribution of HbVs to facilitated O_2 transport could explain the similar O_2 release rates for HbVs (250 nm) and RBCs (8 μm). Under conditions with little facilitated O_2 transport for both HbV and RBC suspensions, only the O_2 affinity (P_{50} value) would be the determining factor for the O_2 release rate, because the P_{50} values for HbVs and RBCs were the same (28 Torr) in the present study. This speculation has to be confirmed in a future study of HbVs and RBCs with different P_{50} values.

Experiments of Page et al. (*experiment A;* Ref. 20) and ours (*experiment B*) showed the enhancement of O_2 unloading by addition of acellular Hb solutions. However, there are some discrepancies between the two groups. *Experiment A* showed that the addition of only 10 vol% of Hb solution to the RBC suspension enhanced O_2 release, whereas in *experiment B*, significant enhancement was observed with addition of 50 vol% of Hb solution, and enhancement was hardly observed for addition of 10 vol% of Hb solution. Furthermore, the reduction of So_2 in *experiment A* was much faster than in *experiment B* despite the identical Hb concentration (10 g/dl) and similar tube diameter (25 μm). For example, the 60% So_2 level of RBCs was attained after 100 s and 100 mm of traveling in *experiment B*, whereas the same So_2 level was attained after <0.2 s and only 4 mm of traveling distance in *experiment A*; the flow velocity was much faster in *experiment A* (~30 mm/s) than in *experiment B* (1.0 mm/s).

These differences between *experiments A* and *B* may be explained as follows. *1*) O_2 permeability of microflow channels: the silicone tube has a higher O_2 permeability [~1,000–6,000 × $cm^3(STP)\cdot cm^{-2}\cdot cm^{-1}\cdot s^{-1}\cdot mmHg^{-1} \times 10^{10}$] compared with the fluorinated ethylenepropylene copolymer tube [59 × $cm^3(STP)\cdot cm^{-2}\cdot cm^{-1}\cdot s^{-1}\cdot mmHg^{-1} \times 10^{10}$] used in *experiment B*. Thus the silicone tube extracts O_2 from the RBC suspension very rapidly by exposure to the deoxygenated environment. *2*) Temperature: *experiment A* was conducted at 37°C, whereas *experiment B* was performed at 25°C. The higher temperature results not only in a higher P_{50} value (22) but also in more facilitation of the process of O_2 unloading in *experiment A*. *3*) Flow velocity: measurements in *experiment B* were carried out when the RBC flow and oxygenation attained steady state at a flow velocity of 1 mm/s. However, the measured So_2 of the flowing RBCs at an observation point showed the RBCs to be in the process of O_2 unloading. In this condition, the measured So_2 would be higher than in the RBC-O_2 equilibrium state. The O_2 distribution in the tube has a parabolic shape; therefore, O_2 is transferred from the centerline toward the wall of the tube. Such an O_2 gradient in the tube may be more prominent at a higher flow velocity and with higher O_2 permeability of the tube as in *experiment A*, as there would be less time for O_2 unloading. Conversely, the thicker marginal RBC-free layer formed at the faster flow velocity may make the Hb-induced facilitation of O_2 release more evident. *4*) Measurement of So_2: in *experiment B*, So_2 was measured on a 5-μm-diameter spot over the centerline of the narrow tube in which O_2 was retained for a longer traveling distance, whereas in *experiment A*, the So_2 was measured for the entire section of the flow channel. However, we confirmed that the So_2 at the center was not significantly different from that at a point a half-radius distance from the center after 100 mm of travel. In relation to the wavelength for the spectroscopy, the measurement in the Soret band (400–450 nm) in *experiment A* was remarkably influenced by the light scattering of the RBCs. On the other hand, the measurement in the Q band with a longer wavelength in *experiment B* was less influenced by the light scattering. These differences in spectroscopy do not seem to provide any quantitative differences in the O_2 release rate. In conclusion, the quantitative difference between O_2 release in *experiments A* and *B* is mainly due to the difference in the O_2 permeability of the flow channels and partly due to the differences in temperature and flow velocity.

It has been suggested that faster O_2 unloading from the HBOCs is advantageous for tissue oxygenation (20). However, this concept is controversial with regard to the recent findings, because an excess O_2 supply would cause autoregulatory vasoconstriction and microcirculatory disorders (1, 23, 41). We confirmed that HbVs do not induce vasoconstriction and hypertension. This is not only owing to the reduced inactivation of nitric oxide as an endothelium-derived vasorelaxation factor (24) but also possibly due to the moderate O_2 release rate that is similar to RBCs as confirmed in this

study. Very recently, Erni et al. (9, 12) demonstrated that HbVs suspended in dextran effectively oxygenated ischemic collaterized tissue in skin flaps. This phenomenon should be explained by the functional characteristics of HbVs; namely, HbV suspension continues to retain O_2 in upstream vessels and reaches the ischemic tissue to release the O_2 (9, 12). In this regard, it is expected that HbVs with a lower P_{50} value would show much slower O_2 unloading, which would be advantageous for ischemic tissue oxygenation. Moreover, the higher viscosity and the resulting higher perfusion pressure (as shown in Fig. 3) would be beneficial to increase the shear stress on the vascular wall for vasorelaxation and to homogeneously transmit the pressure to the microvascular network and thus supply blood to whole capillaries (39). Our experimental results contribute importantly to the design and optimization of O_2 carriers and suggest the possible utilization of HbVs for new clinical indications other than blood substitution.

The authors are grateful to Dr. N. Tateishi (Ehime University) for setting up the microscope for the measurements and for the computer programming and to Dr. M. Intaglietta (University of California, San Diego) for promoting this study.

DISCLOSURE

This work was supported by Health Sciences Research Grants (Research on Pharmaceutical and Medical Safety, Artificial Blood Project); the Ministry of Health, Labor, and Welfare, Japan, and Grants-in-Aid for Scientific Research from the Japan Society for the Promotion of Science (B12480268); and 21 COE, Practical Nano-Chemistry, from the Ministry of Education, Culture, Sports, Science, and Technology, Japan.

REFERENCES

1. **Baines AD, Adamson G, Wojciechowski P, Pliura D, Ho P, and Kluger R.** Effect of modifying O_2 diffusivity and delivery on glomerular and tubular function in hypoxic perfused kidney. *Am J Physiol Renal Physiol* 274: F744–F752, 1998.
2. **Baker M and Wayland H.** On-line volume flow rate and velocity profile measurement for blood in microvessels. *Microvasc Res* 7: 131–143, 1974.
3. **Bayliss LE.** The flow of RBCs in capillary tubes. Changes in the cell-free marginal sheath with changes in the shearing stress. *J Physiol (Lond)* 175: 1–25, 1965.
4. **Beck MR Jr and Eckstein EC.** Preliminary report on platelet concentration in capillary tube flows of whole blood. *Biorheology* 17: 455–464, 1980.
5. **Bouwer ST, Hoofd L, and Kreuzer F.** Diffusion coefficients of oxygen and hemoglobin measured by facilitated oxygen diffusion through hemoglobin solutions. *Biochim Biophys Acta* 1338: 127–136, 1997.
6. **Chang TMS.** *Blood Substitutes: Principles, Methods, Products, and Clinical Trials.* Basel: Karger, 1997.
7. **Chen N, Nishide H, and Tsuchida E.** Analysis of facilitated oxygen transport in a liquid membrane of hemoglobin. *Bull Chem Soc Jpn* 69: 255–259, 1996.
8. **Coin JT and Olson JS.** The rate of oxygen uptake by human red blood cells. *J Biol Chem* 254: 1178–1190, 1979.
9. **Contaldo C, Schramm S, Wettstein R, Sakai H, Takeoka S, Tsuchida E, Leunig M, Banic A, and Erni D.** Improved oxygenation in ischemic hamster flap tissue is correlated with increasing hemodilution with Hb vesicles and their O_2 affinity. *Am J Physiol Heart Circ Physiol* 285: H1140–H1147, 2003.
10. **Duling BR and Berne RM.** Longitudinal gradients in periarteriolar oxygen tension: a possible mechanism for the participation of oxygen in local regulation of blood flow. *Circ Res* 27: 669–678, 1970.
11. **Ellsworth ML, Ellis CG, Popel AS, and Pittman RN.** Roles of microvessels in oxygen supply to tissue. *News Physiol Sci* 9: 119–123, 1994.
12. **Erni D, Wettstein R, Schramm S, Sakai H, Takeoka S, Tsuchida E, Leunig M, and Banic A.** Normovolemic hemodilution with hemoglobin-vesicle solution attenuates hypoxia in ischemic hamster flap tissue. *Am J Physiol Heart Circ Physiol* 284: H1702–H1709, 2003.
13. **Goda N, Suzuki K, Naito S, Takeoka S, Tsuchida E, Ishimura Y, Tamatani T, and Suematsu M.** Distribution of heme oxygenase isoform in rat liver: topographic basis for carbon monoxide-mediated microvascular relaxation. *J Clin Invest* 101: 604–612, 1998.
14. **Intaglietta M, Johnson PC, and Winslow RM.** Microvascular and tissue oxygen distribution. *Cardiovasc Res* 32: 632–643, 1996.
15. **Intaglietta M, Silverman NR, and Tompkins WR.** Capillary flow velocity measurements in vivo and in situ by television method. *Microvasc Res* 10: 165–179, 1975.
16. **Kubota K, Tamura J, Shirakura T, Kimura M, Yamanaka K, Isozaki T, and Nishio I.** The behaviour of red cells in narrow tubes in vitro as a model of the microcirculation. *Br J Haematol* 94: 266–272, 1996.
17. **Maeda N.** Erythrocyte rheology in microcirculation. *Jpn J Physiol* 46: 1–14, 1996.
18. **McCarthy MR, Vandegriff KD, and Winslow RM.** The role of facilitated diffusion in oxygen transport by cell-free hemoglobins: implications for the design of hemoglobin-based oxygen carriers. *Biophys Chem* 92: 103–117, 2001.
19. **Nishide H, Chen XS, and Tsuchida E.** Facilitated oxygen transport with modified and encapsulated hemoglobin across non-flowing solution membrane. *Artif Cells Blood Substit Immobil Biotechnol* 25: 335–346, 1997.
20. **Page TC, Light WR, McKay CB, and Hellums JD.** Oxygen transport by erythrocyte/hemoglobin solution mixtures in an in vitro capillary as a model of hemoglobin-based oxygen carrier performance. *Microvasc Res* 55: 54–66, 1998.
21. **Phillips WT, Lemen L, Goins B, Rudolph AS, Klipper R, Fresne D, Jerabek PA, Emch ME, Martin C, Fox PT, and McMahan CA.** Use of oxygen-15 to measure oxygen-carrying capacity of blood substitutes in vivo. *Am J Physiol Heart Circ Physiol* 272: H2492–H2499, 1997.
22. **Reeves RB.** The effect of temperature on the oxygen equilibrium curve of human blood. *Respir Physiol* 42: 317–328, 1980.
23. **Rohlfs RJ, Bruner E, Chiu A, Gonzales A, Gonzales ML, Magde D, Magde MD Jr, Vandegriff KD, and Winslow RM.** Arterial blood pressure responses to cell-free hemoglobin solutions and the reaction with nitric oxide. *J Biol Chem* 273: 12128–12134, 1998.
24. **Sakai H, Hara H, Yuasa M, Tsai AG, Takeoka S, Tsuchida E, and Intaglietta M.** Molecular dimensions of Hb-based O_2 carriers determine constriction of resistance arteries and hypertension in conscious hamster model. *Am J Physiol Heart Circ Physiol* 279: H908–H915, 2000.
25. **Sakai H, Horinouchi H, Tomiyama K, Ikeda E, Takeoka S, Kobayashi K, and Tsuchida E.** Hemoglobin vesicles as oxygen carriers: influence on phagocytic activity and histopathological changes in reticuloendothelial system. *Am J Pathol* 159: 1079–1088, 2001.
26. **Sakai H, Masada Y, Horinouchi H, Takeoka S, Kobayashi K, and Tsuchida E.** Hemoglobin vesicles suspended in recombinant human serum albumin for resuscitation from hemorrhagic shock in anesthetized rats. *Crit Care Med.* In press.
27. **Sakai H, Masada Y, Takeoka S, and Tsuchida E.** Characteristics of bovine hemoglobin for the potential source of hemoglobin-vesicles as an artificial oxygen carrier. *J* Biochem 131: 611–617, 2002.
28. **Sakai H, Takeoka S, Wettstein R, Tsai AG, Intaglietta M, and Tsuchida E.** Systemic and microvascular responses to hemorrhagic shock and resuscitation with Hb vesicles. *Am J Physiol Heart Circ Physiol* 283: H1191–H1199, 2002.
29. **Sakai H, Tomiyama K, Masada Y, Takeoka S, Horinouchi H, Kobayashi K, and Tsuchida E.** Pretreatment of serum

containing Hb vesicles (oxygen carriers) to avoid their interference in laboratory tests. *Clin Chem Lab Med* 41: 222–231, 2003.
30. **Sakai H, Tsai AG, Rohlfs RJ, Hara H, Takeoka S, Tsuchida E, and Intaglietta M.** Microvascular responses to hemodilution with Hb vesicles as red cell substitutes: influence of O_2 affinity. *Am J Physiol Heart Circ Physiol* 276: H553–H562, 1999.
31. **Shirasawa T, Izumizaki M, Suzuki YI, Ishihara A, Shimizu T, Tamaki M, Huang F, Koizumi KI, Iwase M, Sakai H, Tsuchida E, Ueshima U, Inoue H, Koseki H, Senda H, Kuriyama T, and Homma I.** Oxygen affinity of hemoglobin regulates O_2 consumption, metabolism, and physical activity. *J Biol Chem* 278: 5035–5043, 2003.
32. **Sou K, Naito Y, Endo T, Takeoka S, and Tsuchida E.** Effective encapsulation of proteins into size-controlled phospholipid vesicles using the freeze-thawing and extrusion. *Biotechnol Progr.* First published 25 July 2003; 10.1021/bp0201004.
33. **Takeoka S, Ohgushi T, Terase K, Ohmori T, and Tsuchida E.** Layer-controlled hemoglobin vesicles by interaction of hemoglobin with a phospholipid assembly. *Langmuir* 12: 1755–1759, 1996.
34. **Tateishi N, Maeda N, and Shiga T.** A method for measuring the rate of oxygen release from single microvessels. *Circ Res* 70: 812–819, 1992.
35. **Tateishi N, Suzuki Y, Cicha I, and Maeda N.** O_2 release from erythrocytes flowing in a narrow O_2-permeable tube: effects of erythrocyte aggregation. *Am J Physiol Heart Circ Physiol* 281: H448–H456, 2001.
36. **Tateishi N, Suzuki Y, Shirai M, Cicha I, and Maeda N.** Reduced oxygen release from erythrocytes by the acceleration-induced flow shift, observed in an oxygen-permeable narrow tube. *J Biomech* 35: 1241–1251, 2002.
37. **Tateishi N, Suzuki Y, Soutani M, and Maeda N.** Flow dynamics of erythrocytes in microvessels of isolated rabbit mesentery: cell-free layer and flow resistance. *J Biomech* 27: 1119–1125, 1994.
38. **Tateishi N, Suzuki Y, Tanaka J, and Maeda N.** Imaging of oxygen saturation and distribution of erythrocytes in microvessels. *Microcirculation* 4: 403–412, 1997.
39. **Tsai AG and Intaglietta M.** High viscosity plasma expanders: volume restitution fluid for lowering the perfusion trigger. *Biorheology* 38: 229–237, 2001.
40. **Tsai AG, Johnson PC, and Intaglietta M.** Oxygen gradients in the microcirculation. *Physiol Rev* 83: 933–963, 2003.
41. **Tsai AG, Kerger H, and Intaglietta M.** Microcirculatory consequences of blood substitution with αα-hemoglobin. In: *Blood Substitutes: Physiological Basis of Efficacy*, edited by Winslow RM, Vandegriff K, and Intaglietta M. Boston, MA: Birkhauser, 1995, p. 155–174.
42. **Tsuchida E, ed.** *Blood Substitutes: Present and Future Perspectives.* Amsterdam: Elseviser, 1998.
43. **Vadapalli A, Goldman D, and Popel AS.** Calculations of oxygen transport by red blood cells and hemoglobin solutions in capillaries. *Artif Cells Blood Substitutes Immobilization Biotechnol* 30: 157–188, 2002.
44. **van Assendelft OR.** *Spectrophotometry of Haemoglobin Derivatives.* Assen, The Netherlands: Royal Vangorcum, 1970.
45. **Vandegriff KD and Olson JS.** The kinetics of O_2 release by human red blood cells in the presence of external sodium dithionite. *J Biol Chem* 259: 12609–12618, 1984.

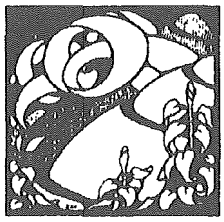

Prolonged Oxygen-Carrying Ability of Hemoglobin Vesicles by Coencapsulation of Catalase in Vivo

Yuji Teramura, Hideo Kanazawa, Hiromi Sakai, Shinji Takeoka, and Eishun Tsuchida*

Advanced Research Institute for Science and Engineering, Waseda University, Tokyo 169-8555, Japan
Received April 23, 2003; Revised Manuscript Received August 21, 2003

Hemoglobin (Hb) vesicles (particle diameter, ca. 250 nm) have been developed as Hb-based oxygen carriers in which a purified Hb solution is encapsulated with a phospholipid bilayer membrane. The oxidation of Hb to nonfunctional ferric Hb (metHb) was caused by reactive oxygen species, especially hydrogen peroxide (H_2O_2), in vivo in addition to autoxidation. We focused on the enzymatic elimination of H_2O_2 to suppress the metHb formation in the Hb vesicles. In this study, we coencapsulated catalase with Hb within vesicles and studied the rate of metHb formation in vivo. The Hb vesicles containing 5.6×10^4 unit mL^{-1} catalase decreased the rate of metHb formation by half in comparison with Hb vesicles without catalase. We succeeded in prolonging the oxygen-carrying ability of the Hb vesicle in vivo by the coencapsulation of catalase.

INTRODUCTION

Ferrous hemoglobin (Hb) reversibly binds oxygen molecules to carry oxygen to terminal tissues and is gradually autoxidized to nonfunctional ferric Hb (metHb). In red blood cells, reduction systems such as NADH–cytochrome b_5, NADPH–flavin, glutathione, and ascorbic acid reduce metHb to ferrous Hb. Superoxide dismutase (SOD) and catalase exist in the cell to eliminate the superoxide anion ($O_2^{-\bullet}$) and hydrogen peroxide (H_2O_2), respectively, and the percentage of metHb in red blood cells is normally maintained at less than 1.0% (*1*, *2*).

At present, several hemoglobin (Hb)-based oxygen carriers, which have been developed as red blood cell substitutes (*3*–*5*), are generally classified into two types: one is the acellular-type modified Hb molecules such as intramolecularly cross-linked Hb (*6*), recombinant cross-linked Hb (*7*), intermolecularly polymerized Hb (*8*), and poly(ethylene glycol) (PEG)-conjugated Hb (*9*). The other is a cellular-type Hb such as Hb vesicles (*10*) or liposome-encapsulated Hb (*11*), in which Hb molecules are encapsulated with a phospholipid bilayer membrane. Some of the acellular-type Hb modifications have advanced to phase III clinical trials (*12*, *13*). Though the Hb vesicles have not yet been clinically studied, their excellent oxygen-carrying ability and high safety have been confirmed in vivo (*10*, *14*–*19*).

When using Hb-based oxygen carriers, the oxidation of ferrous Hb to metHb is an important issue (*20*). Enzymes such as SOD and catalase, and enzymes in metHb reduction systems have been used to limit the metHb formation (*21*, *22*). In the case of acellular Hb, the rate of metHb formation in blood circulation was suppressed compared with that in vitro, because metHb was reduced by reductants contained in the plasma such as ascorbic acid and glutathione. For example, about 40% glutaraldehyde-polymerized bovine Hb was reported to be oxidized to metHb at 72 h after a 90% exchange transfusion in ovines, and no further increase in the metHb percentage was observed (*23*). In the dextran-conjugated Hb, the metHb percentage was maintained at 35%, 12 h after the 50% exchange transfusion in guinea pigs (*24*). On the other hand, in the Hb vesicles, the reductants in plasma are not available because of their low membrane permeability. Among the reactive oxygen species (ROS) such as nitric oxide (NO), $O_2^{-\bullet}$, and H_2O_2, which are known to promote metHb formation, H_2O_2 can permeate through the bilayer membrane, and a relatively large amount of H_2O_2 such as 4–5 μM is constantly generated in normal human plasma (*25*). Therefore, we considered that such exogenous H_2O_2 should be a cause of the metHb formation in addition to the autoxidation of Hb and endogenous H_2O_2 generated by the autoxidation of Hb in the Hb vesicles. Therefore, the metHb formation of Hb vesicles was expected to be suppressed by H_2O_2 elimination.

Although the rate of metHb formation was actually suppressed in vitro by the coencapsulation of catalase, the rate was dramatically increased in vivo. This was because catalase, which was purchased for laboratory use, was contaminated with LPS, and the resulting catalase-coencapsulated Hb vesicles were also highly contaminated with LPS (>10 EU mL^{-1}). We considered that the LPS would promote the rate of metHb formation in vivo because the inflammatory reaction would produce reactive oxygen species. In this study, we prepared the Hb vesicles coencapsulating LPS-free catalase (below 0.1 EU mL^{-1}) and administered the Hb vesicle dispersion to Wistar rats (20 mL kg^{-1}) to study the suppression of the rate of metHb formation by the coencapsulation of catalase.

MATERIALS AND METHODS

1. Removal of Lipopolysaccharide (LPS) from Catalase. A catalase solution (from bovine liver, Sigma, St Louis, MO) was mixed with a 10% Triton X-114 solution (Pierce Chemical, Rockford, IL) and incubated at 4 °C for 30 min. After the mixed solution was incubated at 37 °C for 40 min to separate into two phases, the aqueous phase containing catalase was centrifuged at 5000 rpm for 20 min, and the catalase solution was dialyzed against the water for injection at 4 °C for 24 h.

* To whom correspondence should be addressed. E-mail: eishun@waseda.jp.

10.1021/bc0340619 CCC: $25.00
Published on Web 10/29/2003

The determination of LPS was carried out with limulus assay (Limulus ES−II, Wako Pure Chemical, Osaka). The catalase solution was mixed with the LAL reagent, and the concentration of LPS was determined from the gelation time (Toxinometer ET-201, Wako Pure Chemical). The catalase activity was measured from the decreasing rate of the absorbance at 240 nm when the 0.06% (v/v) H_2O_2 solution (2.9 mL) was mixed with the catalase solution (0.1 mL) at 25 °C.

2. Preparation of Hb Vesicles Coencapsulating Catalase (*26*−*28*). Hb was purified from outdated human red blood cells donated from Japanese Red Cross Blood Center (*27*). After the hemolyzed solution was separated from stromata, the ligand exchange of Hb from O_2 to carbon monoxide (CO) was carried out by CO gas flowing. The proteins other than carbonylHb (HbCO) were denatured by heat treatment (60 °C for 12 h) and removed as precipitates. Pyridoxal 5′-phosphate (PLP, Sigma) as an allosteric effector was added to the HbCO solution (36 g dL^{-1}) at a 2.5:1 molar ratio of PLP to Hb, and the catalase solution was added to it. Mixed lipid [1,2-dipalmitoyl-*sn*-glycero-3-phosphatidylchorine (DPPC, Nippon Fine Chemical, Osaka)/cholesterol (Nippon Fine Chemical)/1,5-dipalmitoyl-L-glutamate-*N*-succinic acid (DPEA, Nippon Fine Chemical)/1,2-distearoyl-*sn*-glycero-3-phosphatidylethanolamine-*N*-PEG (PEG molecular weight was 5000, Sunbright DSPE−50H, H-form, NOF Co., Tokyo), 5/5/1/0.033 by molar ratio] powder was dispersed with the HbCO solution, and the dispersion was stirred at 10 °C for 12 h. The resulting dispersion of multilamellar vesicles was extruded through the membrane filters (FM series, pore size; 3.00, 0.80, 0.65, 0.45, 0.30, 0.22 μm, Fuji Film Co., Tokyo) with a Remolino (Millipore Co., Ltd., Bedford, MA). The Hb vesicles with an average diameter of 250 nm were prepared after extrusion through the membrane filter with 0.22 μm pore size. After the separation of unencapsulated Hb by ultracentrifugation (10000*g*, 60 min), the precipitate of the Hb vesicles was redispersed into saline. Finally, the Hb concentration of the dispersion was adjusted to 10 g dL^{-1}. After Hb vesicles were solubilized with Triton X, the concentration of Hb was determined by a cyanometHb method. In this study, $[catalase]_{fed}$ was defined as the catalase concentration at the mixed solution of Hb and catalase used in the preparation of the Hb vesicles.

The particle diameter of the Hb vesicles was measured by a dynamic light scattering method (N4 PLUS, Beckman Coulter, Fullerton, CA).

3. Measurement of the Rate of metHb Formation of the Hb Vesicle in Vivo. Wistar rats (195−210 g) were used in the experiments. They were anesthetized with diethyl ether, and the Hb vesicle dispersion was administered to the tail vein (20 mL kg^{-1}). The sample was the Hb vesicles coencapsulating catalase (0−5.6 × 10^4 unit mL^{-1}). The blood withdrawn from the tail vein was centrifuged (12000*g*, 5 min) to collect the Hb vesicles in the upper phase of the precipitate. The metHb percentage was calculated based on the intensity ratio at 405 and 430 nm, which were identified as metHb and deoxyHb, respectively, under the nitrogen condition.

RESULTS AND DISCUSSION

The catalase from bovine liver purchased for laboratory use was contaminated with LPS and was not acceptable for in vivo administration. We tried to remove LPS from the catalase solution using a nonionic detergent, Triton X-114. A solution of Triton X-114, which has a cloud point at 20 °C, is homogeneous below this point and is separated into an aqueous phase and a detergent phase above that point (*29*). LPS is highly lipophilic and is transferred from an aqueous phase containing catalase into the organic phase of Triton X-114. We mixed a catalase solution (2.5 × 10^3 unit mL^{-1}) with a Triton X-114 solution (10%, v/v) at 4 °C and separated the mixed solution into two phases at 37 °C to collect the aqueous phase containing catalase. The LPS concentration of the resulting catalase solution was reduced to 0.0038 EU mL^{-1} from >10 EU mL^{-1} without significant dilution. We coencapsulated this purified catalase with Hb in the vesicles.

We then examined the stability of the catalase activity in a solution state at 37 °C. The catalase activities after incubation for 24, 48, and 56 h were 82, 82, and 81%, respectively. The constant activity of around 80% at 37 °C for more than 56 h indicate that the catalase should be tolerable during the in vivo study because the circulation half-life of the Hb vesicles was around 24 h in rats (20 mL kg^{-1}).

The particle diameter of the Hb vesicles was 251 ± 80 nm, and the oxygen affinity (P_{50}) was 30 Torr. For all the Hb vesicles used in this study, oxyHb and metHb were more than 97% and less than 3%, respectively. Neither HbCO nor ferrylHb was detected. After the catalase-coencapsulated Hb vesicles were dissolved by the addition of Triton X, the resulting solution was analyzed by electrophoresis (IEF−PAGE). From the band of catalase, it was confirmed that the catalase was exactly coencapsulated in the Hb vesicles. We tried to measure the catalase activity of the Hb vesicles, however, due to the catalase-like activity of Hb, this activity could not be determined. Therefore, $[catalase]_{fed}$ was defined as the catalase concentration at the mixed solution of Hb and catalase in the preparation process.

The LPS concentration in the resulting Hb vesicle dispersion ([Hb] = 10 g dL^{-1}) was below 0.1 EU mL^{-1}, which was measured by limulus assay after the solubilization of the Hb vesicles with poly(ethylene glycol) 10-lauryl ether (*30*).

We studied the reactivity of the Hb vesicles against ROS ($O_2^{-\bullet}$ and H_2O_2). The rate of $O_2^{-\bullet}$ produced in a 106 μM hypoxanthine/0.32 unit mL^{-1} xanthine oxidase system was 0.9 μM s^{-1}, which was determined by cytochrome *c* (*31*). Catalase was also added to this system to eliminate H_2O_2 from the immediate dismutation of $O_2^{-\bullet}$ ($k = 8.5 \times 10^5$ M^{-1} s^{-1}). As shown in Figure 1a, for the Hb solution, the peaks at 542 and 577 nm, identified as oxyHb, were gradually converted to the peak at 630 nm, identified as metHb, indicating that Hb underwent a one-electron oxidation to metHb by $O_2^{-\bullet}$. On the other hand, in the Hb vesicle dispersion, the UV−vis spectrum, where a large decline in the baseline from the lower wavelength typically shows the turbidity of the vesicles, did not change at all as shown in Figure 1b. This indicated that $O_2^{-\bullet}$ could not permeate through the bilayer membrane due to the electrostatic repulsion from the negatively charged membrane (Figure 1c). Therefore, if the exogenous $O_2^{-\bullet}$ would attack the Hb vesicles, it should have little influence on the metHb formation.

Next, we analyzed the reaction of H_2O_2 with the Hb vesicles as shown in Figure 2a ([heme] = 12 μM, $[H_2O_2]$ = 120 μM); oxyHb was converted to metHb via ferrylHb as an intermediate. In our previous report (*19*), H_2O_2 permeated through the bilayer membrane, and Hb in the vesicles reacted with H_2O_2 in a catalase-like reaction to produce metHb or ferrylHb (Fe^{IV}=O) in the presence of excess H_2O_2. In the case of the Hb vesicles coencapsulating catalase ([catalase] = 4.2 × 10^4 unit mL^{-1}, Figure

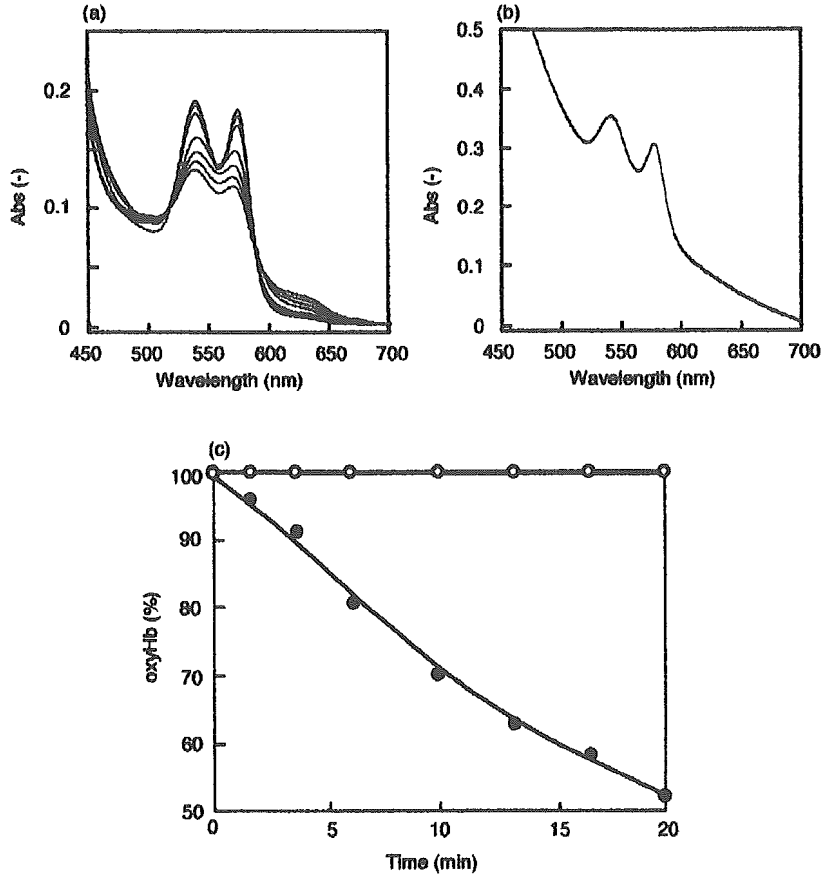

Figure 1. Spectral changes of (a) the Hb solution and (b) the Hb vesicle dispersion ([heme] = 12 μM) during the reaction with $O_2^{-\bullet}$ at 37 °C (0.9 μM s^{-1}). The repeatative scanning was started at a 2 min interval. (c) Changes of the oxyHb in the Hb solution (●) and the Hb vesicle dispersion (○) during the reaction with $O_2^{-\bullet}$.

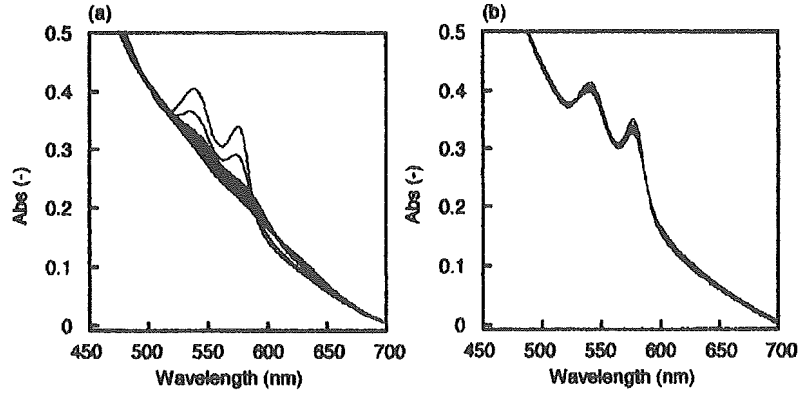

Figure 2. Spectral changes of (a) the Hb vesicle dispersion ([heme] = 12 μM) and (b) catalase-coencapsulating Hb vesicle dispersion ([heme] = 12 μM, $[catalase]_{fed}$ = 4.2 × 10^4 unit mL^{-1}) during the reaction with H_2O_2 at 37 °C. The repetitive scanning was started at a 2 min interval.

2b), a very small amount of oxyHb was converted to metHb without the formation of ferrylHb. This is because the reaction of Hb or catalase with H_2O_2 should be competitive in the vesicles. Most of the H_2O_2 should be eliminated by catalase, and a small amount of H_2O_2 should react with Hb to form metHb (the elimination rate of catalase is about a thousand times greater than that of Hb). We measured the time course of the oxyHb percentage after the addition of 10-fold excess H_2O_2 to oxyHb in the vesicles and calculated the initial decreasing rate of oxyHb (Figure 3). The Hb vesicles without catalase showed a decreasing rate of 42% min^{-1}, whereas the Hb vesicles with catalase showed a lower decreasing rate, depending on the concentration of catalase ($[catalase]_{fed}$). The rate decreased to 5.0% min^{-1} when more than 5.0 × 10^4 unit mL^{-1} was coencapsulated within the vesicle. In this case, the ratio of Hb to catalase was calculated to be 35. We confirmed that the metHb formation of the Hb vesicles by exogenous H_2O_2 could be effectively suppressed by catalase-coencapsulation.

We next examined the catalase encapsulation effect on the autoxidation-derived H_2O_2, namely endogenous H_2O_2. We measured the rate of metHb formation in the Hb vesicles at 40 Torr of oxygen partial pressure (PO_2) in

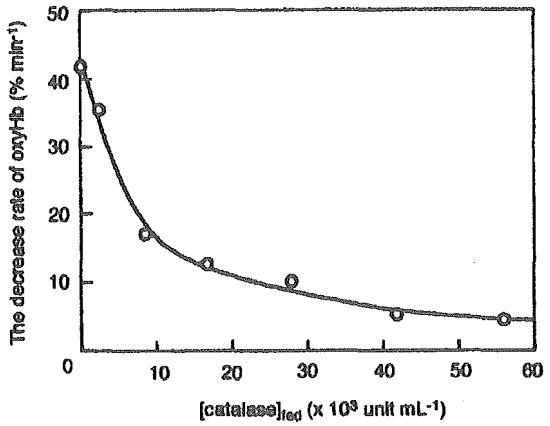

Figure 3. The relationship between the decrease rate of oxyHb in the vesicle ([heme] = 12 μM) and the coencapsulated catalase during the reaction with H_2O_2 ([H_2O_2] = 120 μM).

vitro. When the PO_2 is approximately the P_{50} of Hb, the rate of metHb formation tends to show a maximum (*32*, *33*), and the average oxygen partial pressure in mixed venous blood is estimated to be 40 Torr. Therefore, we used the constant oxygen partial pressure of 40 Torr to measure the rate of metHb formation of the Hb vesicle dispersion for estimation of the in vivo behavior. As shown in Figure 4a, the rate of metHb formation in the Hb vesicles was 3.5% h^{-1}, and in the case of the catalase-coencapsulating Hb vesicles, the rate of metHb formation was significantly reduced from 2.8 to 2.0% h^{-1} with an increase in the encapsulated catalase concentration from 2.8×10^3 to 1.7×10^4 unit mL^{-1}. However, the rate of metHb formation was not reduced even when 2.0×10^4 unit mL^{-1} catalase was coencapsulated (Figure 4b). Inside the vesicle, Hb is autoxidized to metHb with the production of $O_2^{-\bullet}$, and the resulting $O_2^{-\bullet}$ immediately caused a one-electron oxidation of Hb to metHb and the $O_2^{-\bullet}$ became H_2O_2. On the other hand, the $O_2^{-\bullet}$ was immediately dismutated to H_2O_2. As previously reported, the resulting endogenous H_2O_2 also autoxidizes Hb to metHb, or metHb via ferrylHb. Therefore, the autoxidation of Hb should trigger a further oxidation accompanied by the production of reactive oxygen species. In fact, in the group of catalase-coencapsulating Hb vesicles, the reduction of the metHb formation rate indicates that the metHb formation was suppressed by the elimination of the endogenous H_2O_2. The 2.0% h^{-1} rate of metHb formation of the Hb vesicles coencapsulating more than 1.7×10^4 unit mL^{-1} catalase showed that the metHb formation by H_2O_2, which was produced by the autoxidation of Hb in the vesicle, could be completely suppressed by catalase.

It is expected that SOD, which dismutates two $O_2^{-\bullet}$ and two H^+ to H_2O_2 and O_2, should contribute to the reduction of the metHb formation rate. In the Hb solution ([Hb] = 2.0 g dL^{-1}) containing SOD (2.0×10^3 unit mL^{-1}) and catalase (2.0×10^4 unit mL^{-1}), the rate of the metHb formation at 37 °C under atmospheric conditions was 1.3% h^{-1}, which was reduced to 74% compared with a bare Hb solution (1.8% h^{-1}). However, the rate was almost the same as that of the Hb solution containing catalase (1.4% h^{-1}, [catalase] = 2.0×10^4 unit mL^{-1}). From this experiment, we used only catalase as an effective prolongation tool of the Hb function in the Hb vesicles.

To study the rate of the metHb formation in vivo, the Hb vesicles were injected into the rat tail vein (20 mL kg^{-1}). It was confirmed that the LPS concentration in

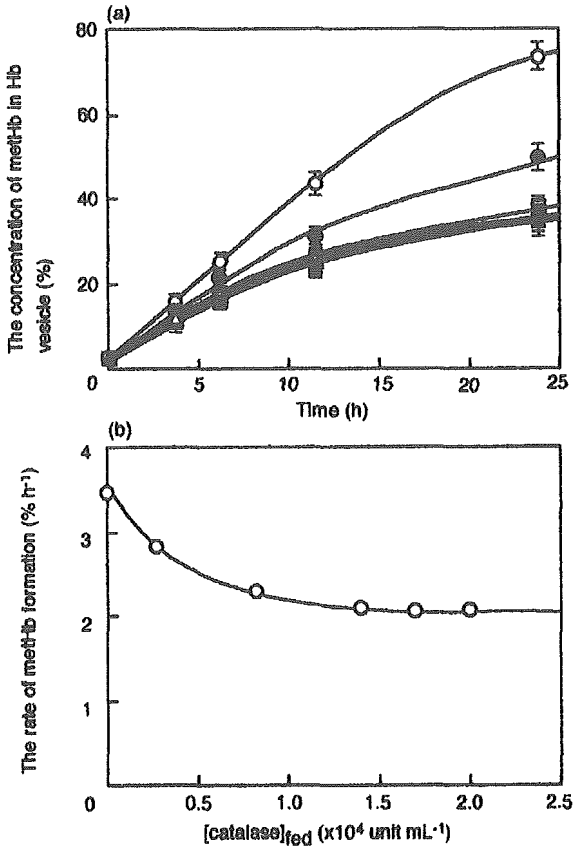

Figure 4. (a) Changes of metHb percentage in the Hb vesicles at 40 Torr of oxygen partial pressure ([Hb] = 2.0 g dL^{-1}). The control is catalase-free Hb vesicles (○). The encapsulated catalase in the Hb vesicle was 2.8×10^3 (●), 8.4×10^3 (□), 1.4×10^4 (■), 1.7×10^4 (△), and 2.0×10^4 unit mL^{-1} (▲). (b) The relationship between $[catalase]_{fed}$ and the rate of metHb formation.

these samples was below 0.1 EU mL^{-1}, approved for in vivo administration. If LPS-contaminated Hb vesicles were injected, the rate of metHb formation should dramatically increase. In the catalase-coencapsulated Hb vesicles ([catalase] = 2.8×10^4 unit mL^{-1}), where the LPS concentration was 10 EU mL^{-1}, the rate of metHb formation was 8.0% h^{-1} (dotted line in Figure 5a), whereas the rate was 2.9% h^{-1} in the catalase-coencapsulated sample of which the LPS concentration was 0.1 EU mL^{-1}. LPS is a major constituent of the outer envelope of Gram-negative bacteria; therefore, it is an extremely potent stimulator of the mammalian immune system and causes the activation of macrophages (*34*, *35*), which should increase the rate of metHb formation by elevation of the reactive oxygen species concentration such as H_2O_2. In this case, there was no effect of the encapsulation with catalase in the Hb vesicles. The effect of such inflammation should exceed the effect of catalase coencapsulation. Therefore, we used the samples where the LPS concentration was below 0.1 EU mL^{-1} in order to accurately measure the rate of metHb formation. In the catalase-free Hb vesicles, the rate of the metHb formation was 3.4% h^{-1}, and the time for 50% metHb formation ($T_{50\%metHb}$) was 14 h. On the other hand, in the groups of catalase-coencapsulated Hb vesicles ([catalase] = 2.8×10^3, 8.4×10^3, 1.7×10^4, 2.8×10^4, 4.2×10^4, and 5.6×10^4 unit mL^{-1}), the rates of metHb formation were 2.9, 2.3, 2.0, 1.8, 1.7, and 1.7% h^{-1}, respectively, and the $T_{50\%metHb}$ were 18, 22, 29, 36, 38, and 39 h, respectively. Figure 5a

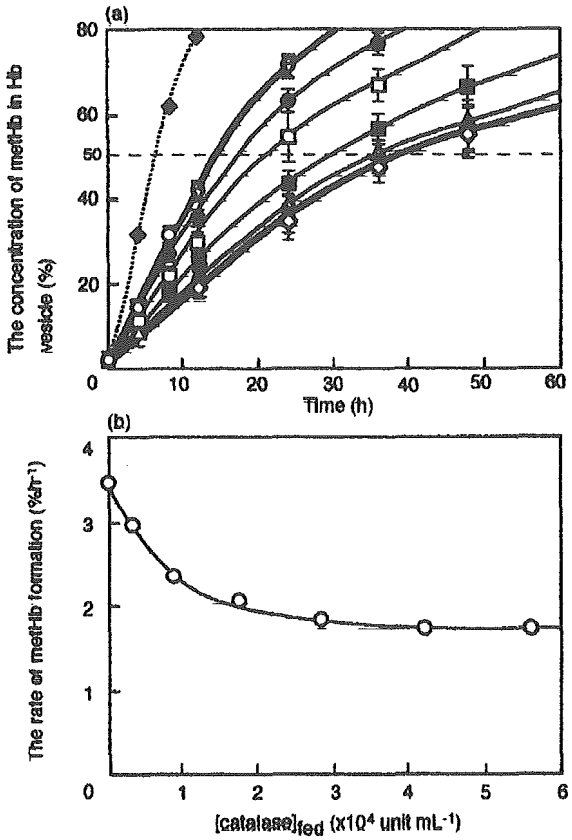

Figure 5. (a) Changes of metHb percentage in the Hb vesicles in vivo (20 mL kg^{-1}, Wistar rat). The control is catalase-free Hb vesicles (○) and the mixture of the Hb vesicle dispersion and the catalase solution (5.6×10^4 unit mL^{-1}, ▽). The encapsulated catalase in the Hb vesicle was 2.8×10^3 (●), 8.4×10^3 (□), 1.7×10^4 (■), 2.8×10^4 (△), 4.2×10^4 (▲), and 5.6×10^4 unit mL^{-1} (◇). The dotted line (◆) is the LPS-contaminated Hb vesicles ([catalase] = 2.8×10^4 unit mL^{-1}). (b) The relationship between $[catalase]_{fed}$ and the rate of metHb formation.

showed the changes in the metHb concentration, indicating that the rest of metHb in the Hb vesicles was the functional ferrous Hb (oxyHb). In the case of the administration of the mixture of the catalase-free Hb vesicle dispersion and catalase solution (5.6×10^4 unit mL^{-1}), there was no significant difference from the control groups (catalase-free Hb vesicles) as shown in Figure 5a. These results showed that the administered catalase rapidly disappeared from the blood stream and could not eliminate hydrogen peroxide.

It was confirmed that, by catalase-coencapsulation, the rate of metHb formation was reduced and the $T_{50\%metHb}$ was also prolonged. As shown in Figure 5b, the rate of metHb formation was saturated when the catalase concentration was over 4.2×10^4 unit mL^{-1} in comparison with 1.7×10^4 unit mL^{-1} in vitro as shown in Figure 4b. Such a high catalase concentration in vivo suggests that metHb formation should be caused by the exogenous H_2O_2 from the blood circulation in addition to the endogenous H_2O_2. It is indicated that the saturated metHb formation rate should be due to the substantial autoxidation of Hb because of the elimination of endogenous and exogenous H_2O_2.

CONCLUSION

Catalase coencapsulated in the Hb vesicle could eliminate H_2O_2, which was not only produced by the Hb autoxidation in the vesicle but also generated in vivo, and the rate of metHb formation in the Hb vesicle could thus be effectively suppressed by catalase coencapsulation. We succeeded in substantially prolonging the oxygen-carrying ability of the Hb vesicles in vivo by coencapsulating catalase.

ACKNOWLEDGMENT

This work was supported in part by Health and Labor Sciences Research Grants, Research on Pharmaceutical and Medical Safety, Ministry of Health, Labor and Welfare, Japan, Grants in Aid for Scientific Research (B) from the Ministry of Education, Science, Sports, and Culture, Japan (12558112), and 21COE "Practical Nano-Chemistry" from MEXT, Japan. One of the authors (Y.T.) thanks Research Fellowships of the Japan Society for the Promotion of Science for Young Scientists.

LITERATURE CITED

(1) Shikama, K. (1984) A controversy on the mechanism of autoxidation of oxymyoglobin and oxyhemoglobin: oxidation, dissociation, or displacement? *Biochem. J. 223*, 279–280.

(2) Tomoda, A. Yoneyama, T., and Tsuji, A. (1981) Changes in intermediate hemoglobins during autoxidation of hemoglobin. *Biochem. J. 195*, 485–492.

(3) Tsuchida, E., Ed. (1998) *Blood substitutes: present and future perspectives.* Elsevier Science, Amsterdam.

(4) D'Agnillo, F., and Chang, T. M. S. (1998) Polyhemoglobin-superoxide dismutase-catalase as a blood substitute with antioxidant properties. *Nat. Biotechnol. 16*, 667–671.

(5) Riess, J. G., (2001) Oxygen carriers ("blood substitutes") -raison d'etre, chemistry, and some physiology. *Chem. Rev. 101*, 2797–2920.

(6) Przybelski, R. J., Daily, E. K., and Birnbaum, M. L. (1997) The pressor effect of hemoglobin – good or bad? In *Advances in Blood Substitutes: Industrial Opportunities and Medical Challenges* (Winslow, R. M., Vandegriff, K. D., and Intaglietta, M., Eds.) Birkhauser, Boston.

(7) Murray, J. A., Ledlow, A., Launspach, J., Evans, D., Loveday, M., and Conklin, J. L. (1995) The effects of recombinant human hemoglobin on esophageal motor function in humans. *Gastroenterology 109*, 1241–1248.

(8) Gould, S. A., Moore, E. E., Hoyt, D. B., Burch, J. M., Haenel, J. B., Garcia, J., DeWoskin, R., and Moss, G. S. (1998) The first randomized trial of human polymerized hemoglobin as a blood substitute in acute trauma and emergency surgery. *J. Am. Coll. Surg. 187*, 113–122.

(9) McCarthy, M. R., Vandegriff, K. D., and Winslow, R. M. (2001) The role of facilitated diffusion in oxygen transport by cell-free hemoglobins: implications for the design of hemoglobin-based oxygen carriers. *Biophys. Chem. 92*, 103–117.

(10) Sakai, H., Horinouchi, H., Tomiyama, K., Ikeda, E., Takeoka, S., Kobayashi, K., and Tsuchida, E. (2001) Hemoglobin-vesicles as oxygen carriers, Influence on phagocytic activity and histopathological changes in reticuloendothelial system. *Am. J. Pathol. 159*, 1079–1088.

(11) Rudolph, A. S., Sulpizio, A., Hieble, P., MacDonald, V., Chavez, M., and Feuerstein, G. (1997) Liposome encapsulating atenuates hemoglobin-induced vasoconstriction inrabbit arterial segment. *J. Appl. Physiol. 82*, 1826–1835.

(12) Mullon, J., Giacoppe, G., Clagett, C., McCune, D., and Dillard, T. (2000) Transfusions of polymerized bovine hemoglobin in a patient with severe sutoimmune hemolytic anemia. *N. Engl. J. Med. 342*, 1638–1643.

(13) Sloan, E. P., Koenigsberg, M., Gens, D., Cipolle, M., Runge, J., Mallory, M. N., Rodman, G. Jr. (1999) Diaspirin cross-linked hemoglobin (DCLHb) in the treatment of severe traumatic hemorrhagic shock: a randomized controlled efficacy trial. *JAMA 282*, 1857–1864.

(14) Sakai, H., Yuasa, M., Onuma, H., Takeoka, S., and Tsuchida, E. (2000) Synthesis and physicochemical characterization of a series of hemoglobin-based oxygen carriers: objective comparison between cellular and acellular types. *Bioconjugate Chem. 11*, 56−64.

(15) Sakai, H., Hara, H., Yuasa, M., Tsai, A. G., Takeoka, S., Tsuchida, E., and Intaglietta, M. (2000) Molecular dimensions of Hb-based O_2 carriers determine constriction of resistance arteries and hypertension in conscious hamster model. *Am. J. Physiol. (Heart Circ. Physiol.) 279*, H908=H915.

(16) Izumi, Y., Sakai, H., Hamada, K., Takeoka, S., Yamahata, T., Kato, R., Nishide, H., Tsuchida, E., and Kobayashi, K. (1996) Physiologic responses to exchange transfusion with hemoglobin vesicles as an artificial oxygen carrier in anesthetized rats: changes in mean arterial pressure and renal cortical tissue oxygen tension. *Circ. Care. Med. 24*, 1869−1873.

(17) Sakai, H., Takeoka, S., Park, S.-I., Kose, T., Izumi, Y., Yoshizu, A., Nishide, H., Kobayashi, K., and Tsuchida, E. (1997) Surface-modification of hemoglobin vesicles with poly(ethylene glycol) and effects on aggregation, viscosity, and blood flow during 90%-exchange transfusion in anesthetized rats. *Bioconjugate Chem. 8*, 15−22.

(18) Kyokane T., Norizumi, S., Taniai, H., Yamaguchi, T., Takeoka, S., Tsuchida, E., Naito, M., Ishimura, Y., and Suematsu, M. (2001) Carbon monoxide from heme catabolism protects against hepatobiliary dysfunction in endotoxin-treated rat liver. *Gastroenterology 120*, 1227−1240.

(19) Takeoka, S., Teramura, Y., Atoji, T., and Tsuchida, E. (2002) Effect of Hb-encapsulation with vesicles on H_2O_2 reaction and lipid peroxidation. *Bioconjugate Chem. 13*, 1302−1308.

(20) Nagababu, E., Ramasamy, S., Rifkind, J. M., Jia, Y., and Alayash, A. I. (2002) Site-specific cross-linking of human and bovine hemoglobins differentially alters oxygen binding and redox side reactions producing rhombic heme and heme degradation. *Biochemistry 41*, 7407−7415.

(21) Chang, T. M. S. (2003) Future generations of red blood cells substitutes. *J. Intern. Med. 253*, 527=535.

(22) Takahashi, A. (1995) Characterization of neo red cells (NRCs), their function and safety in vivo tests. *Artif. Cells Blood Substitutes Immobilization Biotechnol. 23*, 347−354.

(23) Lee, R., Neya, K., Svizzero, T. A., and Vlahakes, G. J. (1995) Limitations of the efficacy of hemoglobin-based oxygen carrying solutions. *J. Appl. Physiol. 79*, 236−242.

(24) Faivre, B., Menu, P., Labrude, P., and Vigneron, C. (1998) Hemoglobin Autoxidation/oxidation mechanism and methemoglobin prevention or reduction processes in the bloodstream. *Artif. Cells Blood Substitutes Immobilization Biotechnol. 26*, 17−26.

(25) Yamamoto, Y., Brodsky, M. H., Baker, J. C., and Ames, B. N. (1987) Detection and characterization of lipid hydroperoxides at picomole levels by high-performance liquid chromatography *Anal. Biochem. 160*, 7−13.

(26) Takeoka, S., Ohgushi, T., Terase, K., Ohmori, T., and Tsuchida, E. (1996) Layer-controlled hemoglobin vesicles by interaction of hemoglobin with a phospholipid assembly. *Langmuir 12*, 1755−1759.

(27) Sakai, H., Takeoka, S., Yokohama, H., Seino, Y., Nishide, H., and Tsuchida, E. (1993) Purification of concentrated hemoglobin using organic solvent and heat treatment. *Protein Expr. Purif. 4*, 563−569.

(28) Sou, K., Naito, Y., Endo, T., Takeoka, S., and Tsuchida, E. (2003) Effective encapsulation of proteins into size-controlled phospholipid vesicles using freeze-thawing and extrusion. *Biotechnol. Prog. 19*, 1547−1552.

(29) Bordier, C. (1981) Phase separation of integral membrane proteins in Triton X-114 solution. *J. Biol. Chem. 256*, 1604−1607.

(30) Sakai, H., Hisamoto, S., Fukutomi, I., Sou, K., Takeoka, S., and Tsuchida, E. (2004) Detection of lipopolysaccharide in hemoglobin-vesicles by Limulus Amebocyte test with kinetic-turbidimetric gel clotting analysis and pretreatment of surfactant. *J. Pharm. Sci.*, in press.

(31) McCord, J. M., and Fridovich, I (1969). Superoxide dismutase. An enzymic function for erythrocuprein (hemocuprein). *J. Biol. Chem. 244*, 6049=6055.

(32) Levy, A., Zhang, L., and Rifkind, J. M. (1988) Hemoglobin: a source of superoxide radical under hypoxic conditions. *Oxy Radicals Mol. Biol. Pathol., Proc. Upjohn-UCLA Symp.*, 11−25.

(33) Mansouri, A., and Winterhalter, H. (1973) Nonequivalence of chains in hemoglobin oxidation. *Biochemistry 12*, 4946=4949.

(34) Raetz, C. R. (1990) Biochemistry of endotoxins, *Annu. Rev. Biochem. 59*, 129=170.

(35) Wright, S. D., Ramos, R. A., Tobias, P. S., Ulevitch, R. J., and Mathison, J. C. (1990) CD14, a receptor for complexes of lipopolysaccharide (LPS) and LPS binding protein. *Science 249*, 1431−1433.

BC0340619

Effective Encapsulation of Proteins into Size-Controlled Phospholipid Vesicles Using Freeze–Thawing and Extrusion

Keitaro Sou, Yoshiyasu Naito, Taro Endo, Shinji Takeoka, and Eishun Tsuchida*

Advanced Research Institute for Science and Engineering, Waseda University, Tokyo 169-8555, Japan

We are aiming to improve the encapsulation efficiency of proteins in a size-regulated phospholipid vesicle using an extrusion method. Mixed lipids (1,2-dipalmitoyl-*sn*-glycero-3-phosphatidylcholine (DPPC), cholesterol, 1,5-dipalmitoyl-L-glutamate-*N*-succinic acid (DPEA), and 1,2-distearoyl-*sn*-glycero-3-phosphoethanolamine-*N*-[monomethoxy poly(ethylene glycol) (5,000)] (PEG-DSPE) at a molar ratio of 5, 5, 1, and 0.033 were hydrated with a NaOH solution (7.6 mM) to obtain a polydispersed multilamellar vesicle dispersion (50 nm to 30 μm diameter). The polydispersed vesicles were converted to smaller vesicles having an average diameter of ca. 500 nm with a relatively narrow size distribution by freeze–thawing at a lipid concentration of 2 g dL^{-1} and cooling rate of −140 °C min^{-1}. The lyophilized powder of the freeze–thawed vesicles was rehydrated into a concentrated protein solution (carbonyl hemoglobin solution, 40 g dL^{-1}) and retained the size and size distribution of the original vesicles. The resulting vesicle dispersion smoothly permeated through the membrane filters during extrusion. The average permeation rate of the freeze–thawed vesicles was ca. 30 times faster than that of simple hydrated vesicles. During the extrusion process, proteins were encapsulated into the reconstructed vesicles with a diameter of 250 ± 20 nm.

Introduction

Vesicles with a lipid bilayer membrane have been vigorously studied as a mimetic model of the biological membrane (*1–3*). The vesicles also have a high potential for application as a carrier of drugs or bioactive macromolecules (such as anti-cancers, enzymes, and functional proteins) in the medical fields (*2, 4–7*). To apply the vesicles in clinical use, we studied the methodology or technology to prepare the vesicles on a large scale according to their purposed performances such as size distribution, encapsulation efficiency, preparation speed, and so on. Phospholipid vesicles encapsulating concentrated Hb (Hb-vesicles, HbV) can be a candidate for oxygen carriers such as red blood cells, having an excellent capability to concentrate atmospheric oxygen and release it in response to a lower partial oxygen pressure (*8–10*). The first HbV was prepared by a film hydration and sonication method in 1980 by Djordjevich et al. (*11*). Several kinds of vesicle preparation methods such as reverse phase evaporation (*12*), detergent removal (*13*), dehydration and rehydration (*14–16*), microfluidization (*17*) or high-speed blending (*18*), and freeze–thawing (*19*) have since been used to encapsulate Hb within vesicles. These preparation methods do not satisfy the precise size control, high encapsulation efficiency, and high yield without causing Hb oxidation and denaturation. Furthermore, the preparation methods using additives such as detergents or organic solvents are undesirable from the safety and environmental viewpoints. We have focused on the development of an extrusion method using isopore membrane filters to control the size of the vesicles without any additives (*20–24*). The drawbacks of the extrusion in a concentrated Hb solution were the slow permeation rate and clogging of the filter pores (*25, 26*). Cullis et al. reported the extrusion of freeze–thawed vesicles in order to more readily prepare the size-controlled vesicles (*27*). Unfortunately, the freeze–thawing process in a concentrated Hb solution had no advantage to improving the extrusion procedure, because the vesicles were cryoprotected by concentrated Hb molecules (40 g dL^{-1}) and the Hb became denatured during the freeze–thawing cycle. Recently, we clarified that the Hb dispersion of the lyophilized powder of the freeze–thawed and poly(ethylene glycol)-modified vesicles very smoothly permeated through a membrane filter. This method could prevent Hb denaturation during the freeze–thawing cycles because freeze–thawing was performed in an Hb-free solution and the lyophilized powder was mixed with the Hb solution before extrusion. In this paper, we report the basic understanding of the effect of the freeze–thawing conditions on size regulation of the vesicles and the effect of the freeze–thawed vesicles on filter permeability and water-soluble protein encapsulation (in this case, Hb) during extrusion in order to prepare size-controlled HbV.

Experimental Procedures

Materials. Powders of 1,2-dipalmitoyl-*sn*-glycero-3-phosphatidylcholine (DPPC) and cholesterol were purchased from Nippon Fine Chemical Co., Ltd., (Osaka, Japan) and 1,2-distearoyl-*sn*-glycero-3-phosphoethanolamine-*N*-[monomethoxy poly(ethylene glycol) (5000)] (PEG-DSPE) was purchased from the NOF Co. (Tokyo, Japan). 1,5-Dipalmitoyl-L-glutamate-*N*-succinic acid (DPEA) was synthesized in our laboratory (*28*). An Hb solution was obtained from outdated donated blood (Japanese Red Cross) according to a previously described

10.1021/bp0201004 CCC: $25.00
Published on Web 07/25/2003

purification method (*29*). The final concentration of the Hb was adjusted to 40 g dL^{-1}.

Preparation of Vesicle Dispersion. DPPC, cholesterol, DPEA, and PEG-DSPE were dissolved in alcohol at a molar ratio of 5, 5, 1, and 0.033 and atomized and evaporated using a spray dryer (Cracks) to prepare a lipid powder at Nippon Fine Chemical Co., Ltd. The mixed lipid powder was dispersed in a NaOH solution (7.9 mM) at 5 g dL^{-1} and hydrated for 2 h to obtain a multilamellar vesicle dispersion. The NaOH concentration was adjusted to be equimolar with DPEA for neutralization. The obtained multilamellar vesicle dispersion was diluted with pure water to the experimental concentrations (1–5 g dL^{-1}). The extruded small vesicles were prepared by passing through the polycarbonate membrane filters in which the final pore size of the filter was 0.1 μm ϕ. The diameter of the resulting vesicles was determined to be 180 ± 15 nm (the size of the vesicles is represented as an average diameter ± standard deviation) using a COULTER submicron particle analyzer (N4SD, Coulter, Hialeah, FL). The extruded large vesicles were prepared by passage through the polycarbonate membrane filters in which the pore size of the filter was 10 μm ϕ. The resulting vesicle dispersion was centrifuged (300*g*, 15 min) to remove the small vesicles in the supernatant. The precipitated vesicles were collected and redispersed into pure water. The diameter of the resulting vesicles was determined to be 3–10 μm.

Freeze–Thawing Treatment. The cooling rate of freezing was strictly controlled using a differential scanning calorimeter (DSC) (Seiko 120 DSC) from −1 to −40 °C min^{-1}. A dispersion (60 μL) of the small or large extruded vesicles was sealed in a silver pan. The pans were placed on the sample stage. The cooling rate and final temperature (−120 °C) was programmed using the included software. After freezing, the pan was kept at 40 °C. The fast freezing (−140 ± 5 °C min^{-1} as an average) was performed by direct dipping of the sealed pan in liquid nitrogen. The thawing was performed by direct dipping of the pan in a 40 °C water bath. The freeze–thawed vesicles were centrifuged (300*g*, 15 min) to precipitate the large vesicles (>3 μm), and the amount of lipids in the supernatant and precipitate was determined by the molibuden blue method (Phospholipid Test Wako; Wako Pure Chem., Tokyo). To obtain the lyophilized powder of the freeze–thawed vesicles, the polydispersed vesicle dispersion (5–25 mL) was sealed in a glass vial, frozen in liquid nitrogen for 3 min, and then thawed in a water bath (40 °C) for 15 min. The resultant vesicle dispersion was frozen in liquid nitrogen for 3 min and dried *in vacuo* using a Bio freeze-dryer (BFD-2F2, Nihonfreezer, Inc., Tokyo, Japan) to obtain the lyophilized powder. The total surface area of the vesicles was measured using 6-*p*-toluidino-2-naphthalene-sulfonic acid (Tns), and the lamellarity of the vesicles was calculated according to our previous paper (*23*).

Sizing and Encapsulation of Hb into Vesicles with Extrusion. The lyophilized powder was dispersed in a concentrated Hb solution (40 g dL^{-1}). After being stirred for 2 h at 25 °C, the dispersion was introduced into an extruder (Lipex Biomembrane, Canada) and extruded through the acetylcellulose membrane filters [FUJI Film Micro Filter; filter pore sizes 3 (FM_3), 0.45 ($FM_{0.45}$), 0.3 ($FM_{0.3}$), and 0.22 μm ($FM_{0.22}$), Fuji Photo Film, Tokyo, Japan] by maintaining a nitrogen gas pressure of 20 kgf cm^{-2}. The permeated volume of the dispersion was recorded on videotape, and the rate of the permeation was calculated. The error in this method was estimated to be less than 2%. The unencapsulating Hb was removed by three ultracentrifugations ($10^5 g$, 90 min).

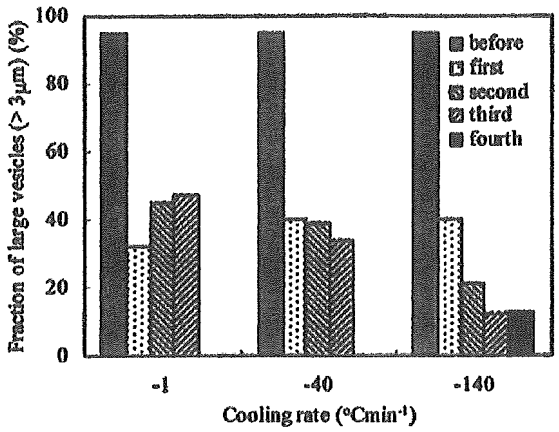

Figure 1. Influence of the cooling rate and number of freeze–thawing cycles on the fragmentation of large vesicles (>3 μm) during freeze–thawing for extruded large vesicles (3–10 μm). The initial vesicular dispersion was prepared by extrusion (10 μm membrane filter pore size), and the small vesicles (<3 μm) were removed by centrifugation. The concentration of the lipids was adjusted to 2 g dL^{-1}.

Determination of Hb and Phospholipid Concentration of the Hb-Vesicles (HbV). The concentrations of the Hb and the phospholipid were determined by a cyanomethemoglobin method (Hemoglobin Test Wako; Wako Pure Chem., Tokyo) and the molibuden blue method, respectively. The encapsulation efficiency of Hb was represented by the weight ratio [Hb]/[lipid].

Results and Discussion

Effect of Freeze–Thawing on Size of Vesicles. The hydrated phospholipid mixture spontaneously formed polydispersed multilamellar vesicles (50 nm to 30 μm diameter). We considered that it was difficult to quantitatively study the effect of freeze–thawing on the size of the vesicles. Therefore, we first studied the change in the size distribution by freeze–thawing treatment for the large (3–10 μm) and small (180 nm) vesicles. To quantify the size distribution of the polydispersed vesicles, we fractionated the large vesicles (>3 μm) by centrifugation (300*g*, 15 min) and determined the phospholipid amount of the fraction. More than 95% of the precipitated vesicles had >3μm diameter, and no small (180 nm) vesicles were precipitated. We roughly determined that the percentage of the precipitation fraction is the large vesicles fraction (>3μm) with less than 5% error. Figure 1 shows the change in the percent of the precipitated fraction (i.e., the large vesicles) after the freeze–thawing cycles. The fraction percent of the large vesicles was 95% before freeze–thawing. After the first freeze–thawing cycle, the percentage of the large vesicles became less than 40% independent of the cooling rate. However, it decreased with the freeze–thawing cycles for the cooling rate of −140 °C min^{-1}. This tendency decreased at −40 °C min^{-1}. When the cooling rate was −1 °C min^{-1}, the percentage was reversibly increased after the second and third freeze–thawing cycles.

The mechanism of the size reduction by freeze–thawing of the large vesicles would be based on breaking the bilayer membrane as a result of dehydration and mechanical pressure accompanied with the growth of ice crystals in the inner and the outer aqueous phases during freezing, and the rehydration of the broken membranes to reconstruct smaller vesicles during thawing (*30, 31*).

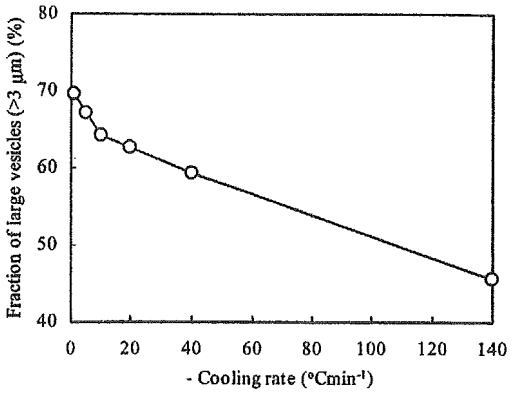

Figure 2. Influence of the cooling rate on the production of fused large vesicles (>3 μm) during freeze–thawing of extruded small vesicles (180 ± 15 nm). The initial vesicular dispersion was prepared by extrusion (0.1 μm membrane filter final pore size) and had no large vesicles (>3 μm).

We confirmed this when the cooling rates were −40 or −140 °C min^{-1}. However, the reverse phenomenon was observed at the cooling rate of −1 °C min^{-1} and could be explained in term of vesicle fusion by freeze–thawing. It is well-known that freeze–thawing is often used for small unilamellar vesicles (SUV) to convert them into large unilamellar vesicles (LUV) by vesicle fusion (*32*). The efficiency of fusion is determined by the average distance between the vesicles, namely, a high vesicle concentration and slow cooling rate result in a short average distance as described below.

We confirmed that the small vesicles (180 ± 15 nm) were fused into larger ones (>3 μm) after the first freeze–thawing cycle, as shown in Figure 2. The percentage of the large vesicles decreased with the increasing cooling rate. The slow cooling rate would result in the growth of large ice crystals, and the local concentration of the vesicles would be increased as a result of the exclusion by ice. Therefore, rehydration should cause the reconstitution of the inter- and intravesicles, namely, fusion. Such fusion should be predominant when small vesicles have been formed by previous preparation, i.e., freeze–thawing of the vesicles.

The mixed lipids formed polydispersed vesicles after hydration in pure water at 5 g dL^{-1}, as shown in Figure 3a. We fractionated the large vesicles (>3 μm) by centrifugation (300*g*, 15 min) and determined that the lipids forming large vesicles occupied 70% of the total lipids. To clarify the influence of the lipid concentration on the freeze–thawing of the polydispersed vesicles, we diluted the large vesicle dispersion (5 g dL^{-1}) with pure water until the concentration of the dispersion became 1, 2, or 3 g dL^{-1}. The diluted samples were frozen at −140 °C min^{-1} and then thawed at 40 °C, and this treatment was repeated three times. As has been estimated, the highly concentrated samples afforded the larger vesicles because fusion would be dominant because of the higher local concentration of the vesicles during freezing. The large vesicle fraction (>3 μm) was reduced to 14% and 13% for the 5 and 3 g dL^{-1} solutions after freeze–thawing, while they were 7% and 6% for the 2 and 1 g dL^{-1} solutions, respectively. The preferable concentration to effectively reduce the large vesicle fraction while considering feasibility in scale was 2 g dL^{-1}. At this condition, the main diameter of the freeze–thawed vesicles was uniformly around 500 nm, as shown in Figure 3b. The conversion of large vesicles to smaller ones and small ones to larger ones as described in Figures 1 and 2 should convert the large vesicles with a wide size distribution to smaller vesicles with a narrow size distribution. The average lamellarity (the number of bilayer membranes) is one parameter to determine the encapsulation efficiency. The efficiency tends to be low for the vesicles having a large lamellarity. Usually, the lamellarity of the vesicles spontaneously formed by conventional lipid hydration is up to 10 (*33*), whereas the average lamellarity of these freeze–thawed vesicles was found to be 2. Therefore, for large polydispersed vesicles, this method was effective not only to regulate the size of the vesicles to ca. 500 nm with a narrow size distribution but also to produce the vesicles with a large encapsulation volume.

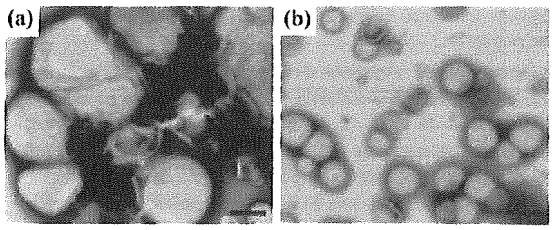

Figure 3. Transmission electron micrographs of the vesicles (a) just after hydration and (b) after three freeze–thawing cycles. Bars represent 500 nm.

Lyophilization of Freeze–Thawed Vesicles and Rehydration in a Hb Solution. The average diameter of the freeze–thawed vesicles as determined by a dynamic light scattering method was 519 ± 78 nm, as shown in Figure 4a. This value was also supported by the size of the vesicles obtained from the TEM observation. The freeze–thawed vesicles were lyophilized in order to replace the water with a concentrated Hb solution. The lyophilized powder was smoothly and homogeneously dispersed and almost restored to the original size of the freeze–thawed vesicles (from 519 ± 78 to 529 ± 100 nm) as compared in Figure 4 b. In general, the lyophilized powder from the vesicle dispersion roughly preserves the vesicle structure, namely, the orientation of the headgroup of the lipids directed toward the surface of the vesicles. However, the rehydrated vesicles tend to become larger and afford a wider size distribution due to fusion. Cryoprotective agents such as saccharides, glycerol, or dimethyl sulfoxide (DMSO) are used to retain the original size and size distribution of the vesicles during the freezing and lyophilizing procedures (*34, 35*). In this experiment, we established cryoprotection by (i) utilization of the freeze–thawed vesicles and (ii) surface modification with PEG. The vesicles prepared by the freeze–thawing repetition to form a steady state should have a resistance to the freezing process. In the lyophilizing process, we froze the sample dispersions under the same condition as the freeze–thawing treatment. In addition, the content of the PEG-lipid was used to reproduce the original size of the freeze–thawed vesicles in an Hb solution. We mixed 0.3 mol % PEG-lipid with the lipid components that were enough to prevent the aggregation of the vesicles (*36–39*). The excluded volume of the PEG chains should prevent the contact between vesicles, to not trigger the aggregation and fusion of vesicles during the lyophilization and rehydration processes. The further incorporation of the PEG-lipid resulted in a significant reduction of the encapsulation efficiency of Hb in the vesicles (*18, 40*). After rehydration with the Hb solution, the encapsulation efficiency of Hb in the resulting vesicles was very low (0.8) as the value of [Hb]/[lipids].